Energy Reports 8 (2022) 13047–13065

Contents lists available at ScienceDirect

Energy Reports

journal homepage: www.elsevier.com/locate/egyr

Research paper

A comparative study of optimization algorithms for parameter estimation of PV solar cells and modules: Analysis and case studies

Mohamed Abdel-Basset [a], Reda Mohamed [a], Marwa Sharawi [b], Laila Abdel-Fatah [a], Mohamed Abouhawwash [c,d,*], Karam Sallam [e]

[a] Department of Computer Science, Faculty of Computers and Informatics, Zagazig University, Zagazig 44519, Egypt
[b] College of Engineering and Applied Sciences, American University of Kuwait, Kuwait
[c] Department of Mathematics, Faculty of Science, Mansoura University, Mansoura 35516, Egypt
[d] Department of Computational Mathematics, Science, and Engineering (CMSE), College of Engineering, Michigan State University, East Lansing, MI 48824, USA
[e] School of IT and Systems, University of Canberra, Canberra, ACT, 2601, Australia

ARTICLE INFO

Article history:
Received 6 April 2022
Received in revised form 5 September 2022
Accepted 28 September 2022
Available online xxxx

Keywords:
Parameter estimation
Nature-inspired algorithm
Solar PV cell/module models
Single-diode Model
Double-diode Model

ABSTRACT

The parameter assessment of solar cells and photovoltaic (PV) modules is a challenging task due to the non-linearity behavior of the current–voltage (I–V) characteristic curve. This paper presents two hybrid nature-inspired algorithms for estimating the unknown parameters of the Single-Diode Model (SDM), and Double-Diode Model (DDM). These algorithms are based on borrowed exploration and exploitation schemes from three well-known optimization algorithms: Whale optimization algorithm (WOA), Marine Predators Algorithm (MPA), and Generalized Normal Distribution Optimization (GNDO) algorithm. The first proposed algorithm is called Marine-Whale-Generalized (MWG) algorithm. In addition, MWG is effectively integrated with novel exploration and exploitation schemes to further its exploration and exploitation operators in a new variant known as (MWGG). A solar cell from RTC France and five commercial PV module models, including Photowatt-PWP201 (PWP), Ultra 85-P (Ultra), and STM6-40/36 (STM), are being used to test the efficacy and efficiency of the proposed algorithms. The experimental findings proved that MWGG is more accurate and faster at convergent results compared to other comparators.

1. Introduction

The sun is a mine of enormous solar energy as it contains almost 173 trillion terawatts which are literally ten thousand more than the world's population uses (Gawusu et al., 2022). In particular, solar energy is produced in the form of heat and light. Therefore, it can be harnessed into heat energy or electricity. Solar heat energy is utilized by concentrated solar power plants (CSP) which produce electricity by using mirrors to heat up a liquid to turn steam turbines or engines connected to a generator. Although the many advantages of CSP, it has fatal disadvantages (Burghard et al., 2022). In other words, the urgent need for water to produce steam makes it an undesirable economic development option. Even though seawater can be considered a potential solution, the operating range of molten salt is limited because it freezes at low temperatures and decomposes at high temperatures.

Solar photovoltaic (PV) power plants are the most popular way to produce electricity based on the photovoltaic effect. In particular, solar cells or diodes convert sunlight into electricity through an electronic process that occurs naturally in certain types of materials known as semiconductors. The light absorption of the solar spectrum is based on the absorption properties of semiconductors. This absorption process causes enough energy to release some negatively charged electrons. In other words, the electrons in these materials are released by stimulating solar rays to travel through electronic circuits connected to the electricity grid (Şevik and Aktaş, 2022). As shown in Fig. 1, solar PV power plants consist of grids of PV modules. Each PV module is a layer of thin-film material that comprises a package of internally series-connected solar cells or diodes. The main advantages of PV modules are that it protects the solar cells from the surrounding environment and delivers a higher voltage than a single solar cell.

As mentioned before, the PV modules and solar cells are significantly responsible for producing electricity from sunlight.

* Corresponding author at: Department of Computational Mathematics, Science, and Engineering (CMSE), College of Engineering, Michigan State University, East Lansing, MI 48824, USA.
E-mail addresses: mohamedbasset@ieee.org (M. Abdel-Basset), redamohamed@zu.edu.eg (R. Mohamed), mamostafa@auk.edu.kw (M. Sharawi), LAShawky@fci.zu.edu.eg (L. Abdel-Fatah), abouhaww@msu.edu (M. Abouhawwash), karam.sallam@canberra.edu.au (K. Sallam).

https://doi.org/10.1016/j.egyr.2022.09.193

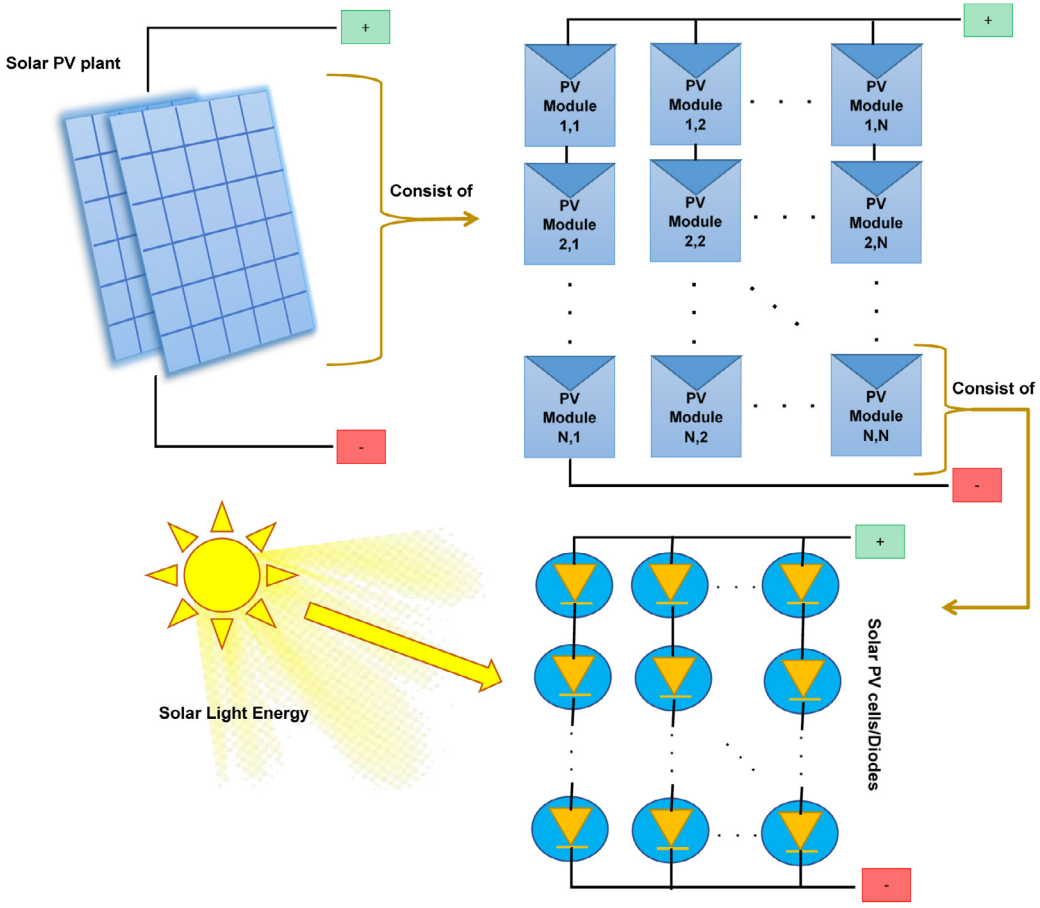

Fig. 1. Solar PV Systems.

Practically, they should acclimate to environmental and climatic changes. Therefore, the parameter estimation of a solar cell is a very important issue as it directly affects the produced electricity (Aboagye et al., 2022). Although many parameters were included in the manufacturer's manual sheet, several parameters are still unknown. There are various methods for estimating these parameters, including analytical, deterministic mathematical, and nature-inspired based methods. The former tries to predict the parameters that stratify the behavior of the current–voltage (I–V) characteristic curve. So, this method is practically inaccurate due to environmental changes. Also, the deterministic mathematical methods are not efficiently applicable as they are exhaustive computational time and are usually trapped into local candidate solutions. Nature-inspired methods or so-called metaheuristics are the most efficient techniques for estimating the unknown parameters of solar cells. Emulating the actions of Artificial Intelligence (AI) is the reason behind the proficiency of these methods.

This paper presents a new Nature-inspired metaheuristic algorithm for estimating the unknown parameters of the Single-Diode Model (SDM) and Double-Diode Model (DDM). This algorithm is based on borrowing some updating schemes from three Nature-inspired metaheuristic algorithms: Whale Optimization Algorithm (WOA), Marine Predators Algorithm (MPA), and Generalized Normal Distribution Optimization (GNDO) algorithm to build a new strongest one enjoying in higher exploration and exploitation; this proposed algorithm is called Marine-Whale-Generalized Algorithm (MWG). In addition, MWG is effectively integrated with novel exploration and exploitation schemes to further improve its exploration and exploitation operators; this new variant is named as MWGG. A solar cell from RTC France and three commercial PV module models, including Photowatt-PWP201 (PWP), Ultra 85-P (Ultra), and STM6-40/36 (STM), are being used to test the proposed algorithm's efficacy and efficiency. The experimental findings proved the promising performance of the proposed algorithms. The main contribution of this study is listed as follows:

- Presenting a new Nature-inspired metaheuristic algorithm based on borrowed some updating schemes from three Nature-inspired metaheuristic algorithms: WOA, MPA, and GNDO algorithm to build a new strongest one for estimating the unknown parameters of SDM and DDM. MWG as the proposed algorithm is a synonym for the Marine-Whale-Generalized algorithm.
- Integrating MWG with novel exploration and exploitation schemes to further improve its exploration and exploitation operators; this new variant is named MWGG.
- The proposed algorithm is a strong alternative to the rival algorithms as the feedback of the experimental outcomes was conducted on several datasets, like a solar cell from RTC France and three commercial PV module models, including PWP, Ultra, and STM.

The rest of the paper is organized as: a literature review is given in Section 2, the Mathematical formulation of the problem is described in Section 3, the proposed algorithm is introduced in Section 4, results and discussion are presented in Section 5, and finally, the conclusion is discussed in Section 6.

Table 1
Nature-Inspired Metaheuristics for Solar Parameter Estimation.

Year	Nature-inspired algorithms	Single diode	Double diode	Three diode	Reference
2018	Teaching–Learning–Based Artificial Bee Colony	✔	✔	–	Chen et al. (2018)
2018	Improved Opposition-Based Whale Optimization Algorithm	✔	✔	✔	Abd Elaziz and Oliva (2018)
2019	Adaptive Differential Evolution Algorithm	✔	✔	–	Biswas et al. (2019); Gong and Cai (2013)
2019	Memetic Adaptive Differential Evolution	✔	✔	–	Li et al. (2019)
2020	Improved Equilibrium Optimizer	✔	✔	✔	Abdel-Basset et al. (2020)
2020	Enhanced Differential Evolutionary Algorithm	–	✔		Shankar et al. (2020)
2020	Orthogonally Adapted Harris Hawks Optimization	✔	✔	–	Jiao et al. (2020)
2020	Coyote Optimization Algorithm	✔	✔	✔	DIab et al. (2020)
2020	Perturbation Mutation Based Particle Swarm Optimization Algorithm	✔	✔	–	Liang et al. (2020)
2021	Whippy Harris Hawks Optimization Algorithm	✔	✔	✔	Naeijian et al. (2021)
2021	ImprovedRao-Based Chaotic Optimization	✔	✔	–	Lekouaghet et al. (2021)
2021	Improved Bonobo Optimizer	✔	✔	✔	Abdelghany et al. (2021)
2021	Adaptive Teaching–Learning-Based Optimization With Experience Learning	✔	✔	–	Mi et al. (2021)
2021	Enhanced Spherical EvolutionAlgorithm	✔	✔	✔	Zhou et al. (2021)
2021	Gaining–Sharing Knowledge-Based Algorithm	✔	✔	✔	Xiong et al. (2021)
2021	Opposition-Based Tunicate Swarm Algorithm	✔	–	–	Sharma et al. (2021)
2021	Improved Marine Predators Algorithm	✔	–	–	Abdel-Basset et al. (2021a)
2022	Jellyfish Search Optimizer	✔	–	–	Bisht and Sikander (2022)
2022	War Strategy Optimization	✔	–	–	Ayyarao and Kumar (2022)
2022	Improved Honey Badger Algorithms	✔	✔	–	Düzenli et al. (2022)
2022	Musical chairs algorithm	✔	✔	–	Eltamaly (2022)
2022	Honey Badger Algorithm	✔	✔	–	Djanssou et al.
2022	Artificial Ecosystem Optimization Algorithm	✔	✔	–	Nguyen et al. (2022)
2022	Tuna Swarm Optimizer	–	–	✔	Kumar and Mary (2022)
2022	Hybrid Particle Swarm Optimization Algorithms	✔	✔	✔	Singh et al. (2022)

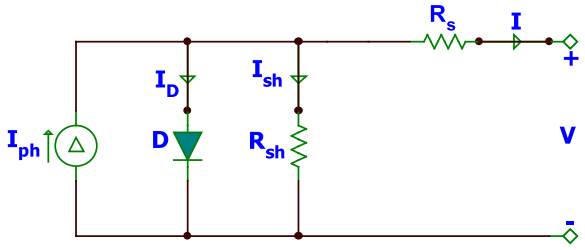

Fig. 2. Equivalent circuit of SDM.

2. Literature review

As shown before, the main engine of the PV-based production of electricity is the PV modules or packages of solar cells. For estimating the unknown parameters of solar cells, various simulations have been proposed for pretending the electrical interoperability of solar PV cells. These simulations range from the Ideal PV cell model to Multi-Dimension Diode Model (Jordehi, 2016). The most common PV cells modeling methods are Single-Diode Model (SDM), and Double-Diode Model (DDM).

Many efforts were made for estimating the unknown parameters of SDM and DDM. Table 1 shows the recently proposed nature-inspired metaheuristics. For instance, Chen et al. (2018) proposed a hybridization between Teaching–Learning-Based Optimization (TLBO) and Artificial Bee Colony (ABC) for estimating the unknown parameters of SDM and DDM. The proposed searching mechanism was divided into three main phases. In addition, it was verified by many commercial models of PV Modules.

Biswas et al. (2019) used the I–V characteristic data at open circuit, short circuit, and maximum power points for problem formulation of the parameters estimation of solar cells. Then, they estimated the unknown parameters of SDM and DDM solar cells by adaptive differential evolution algorithm.

For solving the regarded problem, Jiao et al. (2020) combined original Harris Hawks Optimization (HHO) with orthogonal learning (OL) and general opposition-based learning (GOBL). The proposed algorithm was validated with SDM and DDM. Also in Naeijian et al. (2021), Naeijian et al. introduced an enhanced variant of HHO called Whippy Harris Hawks Optimization (WHHO) for SDM and DDM, and the three-diode model.

Xiong et al. (2021) introduced a new metaheuristic algorithm called the gaining–sharing knowledge-based algorithm. The proposed algorithm was used for estimating the parameters of SDM and DDM. In addition, the proposed algorithm was applied to the three-diode model.

Sharma et al. (2021) proposed an Opposition-Based Tunicate Swarm Algorithm for estimating the parameters of SDM solar cells. Besides, the proposed algorithm was applied to three real PV modules with different numbers of polycrystalline and one monocrystalline.

Abdel-Basset et al. (2021a) improved the performance of the Marine Predators Algorithm (MPA) by adding additional adaptive mutation operation and sorting phases. For verifying the proposed algorithm, SDM and DDM, and many models of PV Modules were used.

Ayyarao and Kumar (2022) proposed a novel metaheuristic called War Strategy Optimization (WSO). The proposed algorithm was inspired by the old war strategy. WSO was validated by estimating the parameters of SDM.

3. Mathematical description of the problem

The solar cell (SC) and PV modules must be designed using a mathematical model that extracts the SC parameters analytically, which must be used in the design process. The SC is modeled using electronic circuits made up of diodes, which are constructed on this basis. The single-diode model (SDM) and double-diode model (DDM) are the most frequently used items for evaluating the parameters of the SC and PV modules, according to the data (Xu and Wang, 2017; DIab et al., 2020).

3.1. Single diode model

As illustrated in Fig. 2, the model contains only one diode, which is used for parallelizing the current source I_{ph}, which is responsible for generating the photo-generated current. The diode performs the function of a half-wave rectifier. Furthermore,

the model takes into account the diode's non-physical ideality factor. Due to the fact that the model has a very straightforward form, it is simple to be implemented. The main problem with this straightforward model is that it includes only five unknown parameters, all of which must be accurately estimated. The equivalent electrical circuit of the SDM is depicted in Fig. 1. In this figure, I_D is the current through the diode and is calculated as follows (Tan et al., 2004):

$$I_D = I_{sd}(\exp\left(\frac{V + I * R_s}{n * V_t}\right) - 1) \tag{1}$$

Where; I_{sd} indicates the reverse saturation current of this diode, V refers to the output cell voltage, R_s considers the series resistance, n is the ideality factor of the diode, and V_t is mathematically defined as:

$$V_t = \frac{k * T}{q} \tag{2}$$

Where; T refers to the temperature degree of the junction in kelvin, k is the Boltzmann constant, $k = 1.3806503 \times 10^{-23}$ J/K, and q defines the electron charge, and $q = 1.60217646 \times 10^{-19}$ C. I_{sh} shown in Fig. 1 is the parallel resistance current and computed according to the following formula:

$$I_{sh} = \frac{V + I * R_s}{R_{sh}} \tag{3}$$

Where R_{sh} is the shunt resistance. Finally, the solar cell current I could be estimated based on the following formula:

$$I = I_{ph} - I_D - I_{sh} \tag{4}$$

From this mathematical model, there are five unknown parameters ($I_{ph}, I_{sd}, n, R_s, R_{sh}$). As a result, accurate estimation of these parameters, which will be performed using different optimization algorithms in the following sections, will be necessary to ensure the proper operation of the model.

3.2. Double diode model

The single diode (SD) model is typically not a good choice for a variety of applications, especially at low irradiance levels, (Djanssou et al.), and as a result, the double diode (DD) model is proposed, as shown in Fig. 3. There are two diodes in Fig. 2; the first serves as a rectifier, and the second is used to take into account the effect of current resulting from the recombination and the impact of non-idealities in the SC. The current balance in the equivalent circuit depicted in Fig. 2 can be represented by the following equation:

$$I = I_{ph} - I_{D1} - I_{D2} - I_{sh} \tag{5}$$

Where I_{D1}, I_{D2} are the currents flowing through the first and second diodes, respectively. The Shockley equivalence is used to update the internal arrangement of the two diodes. Eq. (5) can be reformulated as that:

$$I = I_{ph} - I_{sd1}(\exp\left(\frac{V + I * R_s}{n_1 * V_t}\right) - 1) - I_{sd2}(\exp\left(\frac{V + I * R_s}{n_2 * V_t}\right) - 1) - \frac{V + I * R_s}{R_{sh}} \tag{6}$$

Where; I_{sd1} denotes the first diode current, while I_{sd2} denotes the second diode currents, and n_1 and n_2 denote the ideality factors of the two diodes, respectively. It is clear from Eq. (6) that there are

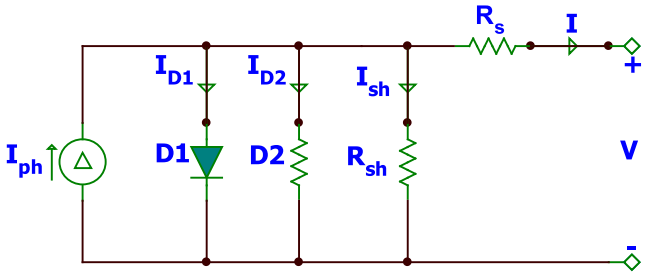

Fig. 3. Equivalent circuit of DDM.

seven unknown parameters ($I_{ph}, I_{sd1}, I_{sd2}, R_s, R_{sh}, n_1, n_2$) that must be precisely estimated in order to accurately design the solar cell.

3.3. Photovoltaic (PV) module

The mathematical models of the SDM and DDM of a photovoltaic module are composed of a series of N_s cells can also be expressed as Eqs. (4) and (6), where $V_t = \frac{N_s kT}{q}$ (Askarzadeh and Rezazadeh, 2012).

4. Proposed algorithms

The algorithm's steps are outlined in detail in the following subsections, which is summarized as initialization, evaluation, generalized normal distribution algorithm, marine predators algorithm, whale optimization algorithm, and additional exploration and exploitation operators, and finally, the proposed algorithms: marine-whale-generalized (MWG) algorithm, and MWG integrated with an additional global operator (MWGG).

4.1. Initialization

The majority of metaheuristic algorithms begin the optimization process by generating an initial population independent of a uniform random distribution. Each agent in the population is referred to as a "vector" and the population consists of N vector agents distributed across a d-dimensional search space by the following formula:

$$\vec{X}_i = \vec{lb} + \left(\vec{ub} - \vec{lb}\right).\vec{r} \tag{7}$$

Where, $\vec{r}$ is a vector containing a value defined at random between 0 and 1. $\vec{lb}$ and $\vec{ub}$ are the lower and upper bounds of the dimensions of the optimization problems. Initially, the proposed algorithm employs these N solutions $\vec{X}_i(i \in N)$, where each solution contains a number of dimensions d equal to the number of unknown parameters that need to be optimized; five dimensions ($I_{ph}, I_{sd}, n, R_s, R_{sh}$) for the SDM and seven dimensions ($I_{ph}, I_{sd1}, I_{sd2}, R_s, R_{sh}, n_1, n_2$). Following initialization, each solution is evaluated using the objective function (OF) described in the following section to determine the quality of each solution in comparison to the other solutions, as well as the solutions obtained within the subsequent generations. The solution representation for five unknown parameters of SDM are represented in Fig. 4 to show clearly to the reader the contents of solutions

I_{ph}	I_{sd}	R_s	R_{sh}	n
0.7694	1.212E-07	0.0433	25.6595	1.3910

Fig. 4. Representation of a solution for SDM.

during the optimization process; the same situation for DDM whose parameters are represented in Fig. 5 as an illustrative example for the initialization process.

4.2. Evaluation phase

The primary goal of solving the parameter extraction problem is to determine the values of the unknown parameters that result in the least amount of error between the measured and simulated current data. Therefore, the root mean squared error (RMSE), refers to as the objective function (OF), is developed to compute the difference between the measured and estimated data according to the following formula:

$$RMSE = OF(X_i) = Min\sqrt{\frac{1}{M} * \sum_{k=1}^{M}(I_k - I_e(V_k, \vec{X}_i))^2} \tag{8}$$

I_k is the measured current, and I_e refers to the estimated current. M indicates the length of the data that was measured. X_i are the estimated parameters of the ith solution. I_e is calculated using the extracted parameters represented in $\vec{X}_i$ and the Newton–Raphson method for tackling Eqs. (4) and (6) as follows (Nunes et al., 2018):

$$I_e\left(V_k, \vec{X}_i\right) = f\left(I_e\left(V_k, \vec{X}_i\right)\right) - \frac{f\left(I_e\left(V_k, \vec{X}_i\right)\right)}{f'\left(I_e\left(V_k, \vec{X}_i\right)\right)} \tag{9}$$

$f'\left(I_e\left(V_k, \vec{X}_i\right)\right)$ is the first derivative of $I_e\left(V_k, \vec{X}_i\right)$ as depicted in Eq. (11) for SDM.

$$f\left(I_e\left(V_k, \vec{X}_i\right)\right) = I_{ph} - I_{sd}\left(\exp\left(\frac{q\left(V_k + I_e\left(V_k, \vec{X}_i\right) * R_s\right)}{nkTN_s}\right) - 1\right) - \frac{V_k + I_e\left(V_k, \vec{X}_i\right) * R_s}{R_{sh}} - I_e\left(V_k, \vec{X}_i\right) \tag{10}$$

$$f'\left(I_e\left(V_k, \vec{X}_i\right)\right) = -I_{sd}\frac{qR_s}{nkTN_s}\left(\exp\left(\frac{q\left(V_k + I_e\left(V_k, \vec{X}_i\right) * R_s\right)}{nkTN_s}\right) - 1\right) - \frac{R_s}{R_{sh}} - 1 \tag{11}$$

4.3. Generalized normal distribution optimization (GNDO)

A generalized normal distribution (GNDO) has recently been proposed as an algorithm for solving nonlinear optimization problems, such as the estimation of solar cell parameters (Zhang et al., 2020). Inspired by normal distribution theory, this algorithm uses two main stages of the optimization process: exploration and exploitation. Exploration occurs when the algorithm searches the search space for the most promising region that may contain the optimal solution. The exploitation process concentrates its efforts on this promising region in order to arrive at the best possible solution. In our work, we employ the exploration operator of GNDO due to its ability to substantially cover the area of the search space of the optimization problem. During the exploration stage, the optimization problem's search space is thoroughly investigated in an attempt to locate the most promising region where the optimal solution may be found. As a result, the following are mathematical formulations of phases:

$$\vec{T}_i^t = \vec{X}_i^t + \beta \times (|\lambda_3| \times v_1) + (1 - \beta) \times (|\lambda_4| \times v_2) \tag{12}$$

λ_3 and λ_4 are numerical values that are generated at random using the standard normal distribution as a basis, β is a numerical value defined randomly at the range 0 and 1. $\vec{v}_1$ and $\vec{v}_2$ are two trial vectors defined by:

$$\vec{v}_1 = \begin{cases} \vec{X}_i^t - \vec{X}_a^t, & if\ f(\vec{X}_i^t) \le f(\vec{X}_a^t) \\ \vec{X}_a^t - \vec{X}_i^t, & otherwise \end{cases} \tag{13}$$

$$\vec{v}_2 = \begin{cases} \vec{X}_b^t - \vec{X}_c^t, & if\ f(\vec{X}_b^t) \le f(\vec{X}_c^t) \\ \vec{X}_c^t - \vec{X}_b^t, & otherwise \end{cases} \tag{14}$$

$a, b,$ and$c$ are indices picked randomly from the solutions, such that $a \neq b \neq c \neq i$. This phase is updated to further improve the performance of the proposed algorithm; our improvement was based on mutating the current solution with the new solution to take into consideration the quality of some dimensions found in the current solution with those found in the new solution. Generally, this improvement is formulated as follows:

$$\vec{T}_i^t = \vec{X}_i^t + (\beta \times (|\lambda_3| \times v_1) + (1 - \beta) \times (|\lambda_4| \times v_2)) \times \vec{Z} \tag{15}$$

$$\vec{Z} = \begin{cases} 1 & \vec{r} \le P_m \\ 0 & Otherwise \end{cases} \tag{16}$$

Where $\vec{r}$ is a vector including numerical values defined at random between 0 and 1. P_m is a predetermined scalar probability to determine the effect of the newly updated dimensions on the current.

4.4. Marine predators algorithm (MPA)

In addition, within our experiments, we found that the fish aggregating devices (FADs) mechanism of MPA has an effect on the performance of the proposed algorithm because it helps in exploring the regions which are intractable for the exploration operator of GNDO discussed previously. This mechanism: FADs affects significantly the performance of MPA. Based on some studies, as a result of FADs, the predators spend 20% of their search time exploring another environment around the search space with abundant prey, while the other time they search for a better solution within the surrounding environment. FADs could be mathematically computed according to the following formula (Faramarzi et al., 2020):

$$\vec{T}_i = \begin{cases} \vec{X}_i + CF[\vec{lb} + \vec{r}_2(\vec{ub} - \vec{lb})] \otimes \vec{U} & if\ r < FADs \\ \vec{X}_i + [FADs\,(1 - r) + r]\left(\vec{X}_a - \vec{X}_b\right) & if\ r \ge FADs \end{cases} \tag{17}$$

$$CF = (1 - \frac{t}{t_{max}})^{\left(2\frac{t}{t_{max}}\right)} \tag{18}$$

Where r is a number generated at random between 0 and 1. $\otimes$ denotes the element by element multiplication, t and t_{max} indicates the current generation and the maximum number of function evaluations, respectively. $\vec{r}_2$ is a vector containing random values ranging from 0 to 1. $\vec{U}$ is a binary vector consisting of the numbers 0 and 1 according to Eq. (19). FADs = 0.2 indicates the likelihood that FADs will have an effect on the optimization process. a, and b indicate the indices of two randomly chosen solutions from the population.

$$\vec{U} = \begin{cases} 1 & \vec{r} \le FADs \\ 0 & Otherwise \end{cases} \tag{19}$$

$I_{ph}(A)$	$I_{sd1}(A)$	$R_s(\Omega)$	$R_{sh}(\Omega)$	n_1	$I_{sd2}(A)$	n_2
0.76077	2.709e-07	0.036561	54.53375	1.826677	2.49e-07	1.460937

Fig. 5. Representation of a solution for DDM.

4.5. Whale optimization algorithm

Mirjalili and Lewis created a computer simulation of the actions and behaviors of humpback whales for proposing a new metaheuristic algorithm known as whale optimization algorithm (WOA). In attack mode, the whales surround their victim in a spiral shape, swimming up to the surface in a shrinking circle, using an incredible feeding method, which is referred to as the bubble-net approach, when attacking their victim or prey. WOA simulates this hunting mechanism by assigning a 50 percent chance of selecting between a spiral model and a shrinking encircling prey in order to generate the new position of the current whale in the current environment. The following mathematical formula simulates the encircling mechanism:

$$\vec{T}_i^t = \vec{X}^* - \vec{A} * \vec{D} \tag{20}$$

$$\vec{A} = 2 * a * rand - a \tag{21}$$

$$a = 2 - 2 * \frac{t}{t_{max}} \tag{22}$$

$$\vec{D} = \left| \vec{C} * \vec{X}^* - \vec{X}_i^t \right| \tag{23}$$

$$\vec{C} = 2 * rand \tag{24}$$

Where $\vec{X}_i^t$ is a vector including the position of the current solution, $\vec{X}^*$ is a vector including the position of the best solution found so far, *rand* is a random number in [0, 1], and a is a distance control parameter linearly decreased from 2 to 0. WOA uses a random solution from the population to update the current whale's position in the search area when searching for prey in a new direction. If $\vec{A}$ is greater than a random number generated between 0 and 1, then a random solution from the population is used to update the current whale. The mathematical model for the exploration phase of the MPA is as follows:

$$\vec{T}_i^t = \vec{X}_{rand}^t - \vec{A} * \vec{D} \tag{25}$$

$$\vec{D} = \left| \vec{C} * \vec{X}_{rand}^t - \vec{X}_i^t \right| \tag{26}$$

Where $\vec{X}_{rand}^t$ is a random position vector chosen from the current population. The encircling mechanism and exploration phase are also employed in the proposed algorithm to achieve two purposes: the first one is exploring the regions around the solution found in the population in the hope that one of these solutions are close to the near-optimal solution which is desired for solving the optimization problem, and the second one is exploiting the regions around the best-so-far solution will help in accelerating the convergence speed towards the near-optimal solution.

4.6. Additional exploration and exploitation operators

Unfortunately, the performance of the proposed algorithm needs more improvements in the exploration operator to keep its stability for various optimization problems. Therefore, an additional exploration operator is added with a probability to the proposed algorithm to further improve its exploration operator for some of the PV modules. The mathematical model of this operator is as follows:

$$\vec{T}_i = \begin{cases} \vec{lb} + \vec{r} \times \left(\vec{X}_a - \vec{X}_b \right) & if\ r < 0.5 \\ \left(\frac{t_{max} - t}{t_{max}} \right) \vec{X}_i + \left(\frac{t}{t_{max}} \right) \vec{X}^* + lv \times \left(\vec{X}_a - \vec{X}_b \right) & if\ r \geq 0.5 \end{cases} \tag{27}$$

Where lv is a Levy flight-based value. $\vec{r}$ is a vector including numerical values ranging between 0 and 1. $\vec{X}_a$ and $\vec{X}_b$ are two solutions selected randomly from the current population. As discussed before, the majority of employed operators support the exploration operator, and hence the proposed algorithm will be poor for the problem which needs greater exploitation than exploration. Thus, in this study, an additional exploitation operator is added to strengthen the performance of the proposed algorithm. The mathematical model of this operator is as follows:

$$\vec{T}_i = \vec{X}_a + (1 - \delta) \times \left(-\vec{X}_a + \vec{X}^* \right) \tag{28}$$

$$\delta = e^{-\tau r \frac{t}{t_{max}}} \tag{29}$$

Where τ is an exploitation factor to determine the change rate in the generated step size. Increasing this factor reduces the movements toward the best-so-far solution and hence reduces the exploitation operator of the proposed algorithm. This operator is estimated later in the experiments section.

4.7. MWG and MWGG

This section shows the way of integrating various updating schemes discussed in the previous sections to propose a new metaheuristic algorithm able to find the unknown parameters of the SDM and DDM. These schemes are together integrated based on a control factor p which is generated according to the current function evaluation, where at the start of the optimization process, this factor is near 1 and reduces gradually even reaching 0. The mathematical model of this parameter is as follows:

$$p = \left(\frac{t_{max} - t}{t_{max}} \right) \tag{30}$$

The optimization process of the proposed algorithm starts updating the solutions according to the schemes of WOA to cover regions within the population, in addition to those around the best-so-far solution to accelerate the convergence speed in the right direction of the near-optimal solution. Afterward, the FADs of MPA will be fired to explore globally the search space of the optimization problem to avoid getting stuck into local minima, in addition to exploring the regions within the solutions as an attempt to accelerate the convergence speed in the case of existing an near-optimal solution close to them. At the end of the optimization process, the exploration operator of GNDO in addition to the exploitation operator formulated in (28) will be exchanged with each other to find better solutions that are intractable by both FADs and WOA. Finally, the steps of the proposed algorithm called the Marine-Whale-Generalized (MWG) algorithm, which could be also abbreviated to GWM, are clearly listed in Algorithm 1 and depicted in Fig. 6

Algorithm 1 MWG

Initialize a population of N solutions $\vec{X}_i(i = 1,2,3,\ldots,N)$
Evaluate the fitness of each $\vec{X}_i$
Find the best solution $\vec{X}^*$
$t = 1$
while $(t < t_{max})$
  for each i solution
    Update a, A, p, C, and l
    $\boldsymbol{r}$: create a random number between 0 and 1
    if $(r < p)$
      Update $\boldsymbol{r}$
      if $(r < p)$ %% **Whole optimization algorithm**
        Update $\boldsymbol{r}$
        if $(|A| < r)$
          Create $\overrightarrow{T_i^t}$ using (20)
        else
          Create $\overrightarrow{T_i^t}$ using (25)
        end if
      else%% **Marine predators algorithm**
        Create $\overrightarrow{T_i^t}$ using (17)
      else
        $\boldsymbol{r}$: create a random number between 0 and 1
        $\boldsymbol{r_1}$: create a random number between 0 and 1
        if $r < r_1$ %% **Generalized normal distribution**
          Create $\overrightarrow{T_i^t}$ using (15)
        else %% **Additional exploitation operator**
          Create $\overrightarrow{T_i^t}$ using (28)
        end if
    end if
    Evaluate $\overrightarrow{T_i^t}$ and set it in $\overrightarrow{X_i^t}$ if it is better
    Update $\overrightarrow{X^*}$ if there is better.
    t=t+1
  end for
end while

Unfortunately, the performance of MWG is weak for some test cases validated in this study. Therefore, the additional exploration operator formulated in (27) is employed with MWG to further improve its exploration operator to overcome this demerit; this operator is applied with a probability p_e to avoid stuck into local minima. Finally, the proposed algorithm which includes this additional exploration operator is listed in Algorithm 2 and abbreviated as MWGG, or GMWG.

Algorithm 2 MWGG

Initialize a population of N solutions $\vec{X}_i(i = 1,2,3,\ldots,N)$
Evaluate the fitness of each $\vec{X}_i$
Find the best solution $\vec{X}^*$
$t = 1$
while $(t < t_{max})$
  Execute the main steps of MWG listed in **Algorithm 1**
  $\boldsymbol{r}$: create a random number between 0 and 1
  If $(r < p_e \times p)$
    for each i solution
      Create $\overrightarrow{T_i^t}$ using (27)
      Evaluate $\overrightarrow{T_i^t}$ and set it in $\overrightarrow{X_i^t}$ if it is better
      Update $\overrightarrow{X^*}$ if there is better.
      t=t+1
    end for
  end if
end while

5. Results and discussion

This section employs the proposed algorithms: MWGG and MWG to estimate the unknown parameters of two PV models: SDM and DDM for three commercial PV modules, such as Photowatt-PWP201 (PWP), Ultra 85-P (Ultra), and STM6-40/36 (STM), and an RTC France solar cell (Ginidi et al., 2021; Soliman et al., 2020; El-Dabah et al., 2021; Abdel-Basset et al., 2021b; Rezk et al., 2021; Fan et al., 2022; Ayyarao and Kumar, 2022). The characteristics of these PV models are represented in the short-circuit current point (I_{SC}), the open-circuit current–voltage (V_{oc}), the maximum output voltage (V_m), the maximum output power (P_m), the maximum output current (I_m), the number of cells connected in series in PV modules (N_s), the short-circuit current–temperature factor(k_i), and the temperature coefficient of open-circuit voltage (k_v) are presented in Table 2 (Ginidi et al., 2021). In addition, the search boundary of each unknown parameter is presented in the same table.

This study compares the performance of the proposed algorithms: MWG and MWGG with nine well-known state-of-the-art optimization algorithms to show their efficiency; those algorithms are the sine–cosine algorithm (SCA) (Mirjalili, 2016), Marine Predators Algorithm (MPA) (Faramarzi et al., 2020), Grey Wolf Optimizer (GWO) (Mirjalili et al., 2014), Generalized Normal Distribution Optimization (GNDO) (Zhang et al., 2020), African vultures optimization algorithm (AVOA) (Abdollahzadeh et al., 2021b), gorilla troops optimizer (GTO) (Abdollahzadeh et al., 2021a), whale optimization algorithm (WOA) (Xiong et al., 2018), interior search algorithm (ISA) (Gandomi, 2014), equilibrium optimizer (EO) (Abdel-Basset et al., 2020). These compared algorithms have been recently applied to tackle several optimization problems and could achieve significant success in comparison to several heuristics and metaheuristic techniques. The parameters of these algorithms have been chosen in accordance with the cited papers, with the exception of the maximum number of function evaluations and the population size, which have been set to 50,000 and 20 respectively to ensure a fair comparison. For the experiments implemented in this study using Matlab R2019a, a device with the following specifications is used: Intel(R) Core(TM) i7-4700MQ CPU @ 2.40 GHz 2.40 GHz, 32 GB of RAM, and 64-bit Windows 10 Pro. The proposed algorithms have three main effective parameters; these parameters are τ, P_m, and p_e and set to 20, 0.2, and 0.1, respectively, after conducting extensive experiments.

5.1. Comparison over single-diode model (SDM)

In this section, the various improvements employed to build up the proposed algorithm are accurately investigated to show the effectiveness of each one. These improvements are symbolized in Table 3 as follows:

- W: indicates the updating functions Eqs. (20) and (25) of WOA
- G: indicates the updated Eq. (15) borrowed from GNDO
- M: indicates the Eq. (25) borrowed from MPA
- WM: indicates integrating W with M
- GM: integrating G, W, and M
- MWG: indicates integrating GM with the additional exploitation equation represented in (28)
- MWGG: indicates integrating MWG with the additional exploration operator represented in (27)

Each of these variants is independently executed 30 times, and the resulting RMSE values are analyzed in terms of four statistical information: best, average (Ave), worst, and standard deviation (Std), as shown in Table 3. According to the outcomes presented in Table 3 for various test cases under both SDM and DDM, the integrated methods in the proposed algorithm MWGG and MWG have a significant effect on its performance and hence those are beneficial within the proposed.

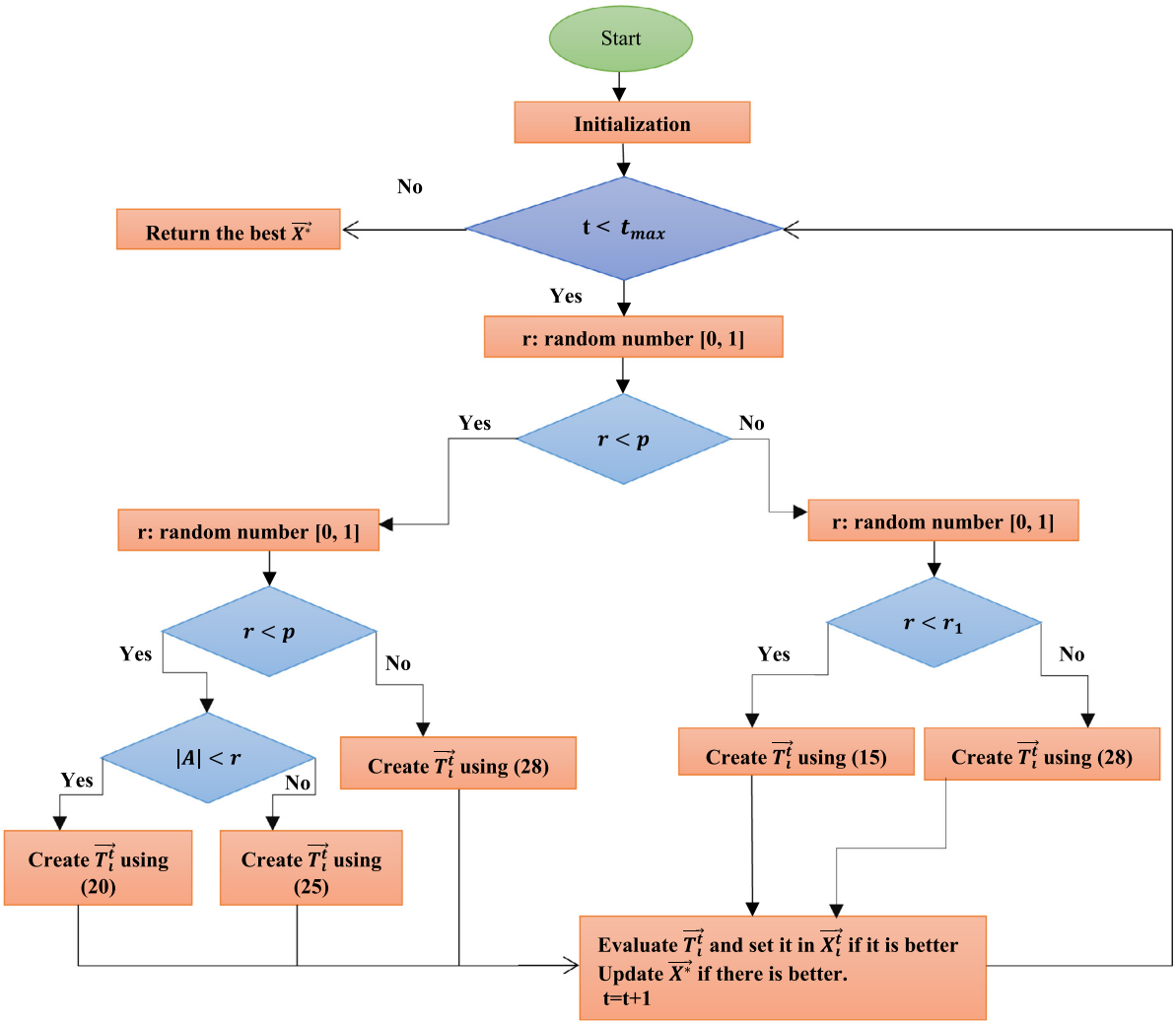

Fig. 6. Flowchart of the proposed algorithm MWG.

Table 2
Characteristics of six observed PV models and search boundaries of unknown parameters.

Characteristics of PV models					Search space of unknown parameters		
Characteristics	**RTC**	**Ultra**	**STM**	**PWP**	**Parameter**	**LB**	**UB**
P_m [W]	0.31	85	25.5	11.5	I_{ph} (A)	$0.9I_{SC}$	$1.1I_{SC}$
V_m [V]	0.459	17.2	16.98	12.649	I_{sdi} (A) , $i \in 1:2$	1 nA	10 μA
I_m [A]	0.6755	4.95	1.5	0.912	R_s (Ω)	0	0.5
V_{oc} [V]	0.5736	22.2	21.02	16.7785	R_{sh} (Ω)	0	500
I_{SC} [A]	0.7605	5.45	1.663	1.0317	$a1$	1	2
N_s	1	36	36	36	$a2$	1.2	2
K_i	0.000387	0.0008	−0.00065	0.0008			
K_v	−0.003739	−0.0725	−0.00346	−0.0725			

5.2. Comparison over single-diode model

This section presents the outcomes obtained by the proposed algorithms and the rival algorithms when solving the SDM over various PV modules and RTC France cells. Our analysis in this section is based on two folds: the first one is the quantitative analysis which analyzes the performance of the algorithms in terms of the best, average (Ave), worst, and standard deviation of RMSE values obtained within 30 independent times, in addition to a *p*-value of the Wilcoxon rank-sum test to determine the difference between the outcomes of the proposed algorithms and these of the rival optimizers; the second fold compares visually the different algorithms in terms of convergence curve, and five-number summary (Boxplot), as well as depicting I–V curves of both measured and estimated data and difference between measured and estimated currents.

5.2.1. Quantitative analysis

This section starts with the quantitative analysis which is based on comparing statistical information (Best, Ave, worst, *p*-value, SD) of the proposed algorithms with these of rival optimizers for three PV modules and a solar cell.

A. **R.T.C France**

Each algorithm is executed in 30 independent runs and its outcomes are analyzed to extract five statistical information: Best, Ave, worst, and SD which is presented in Table 4 along with

Table 3
Comparison of different improvements.

	RTC France (SDM)				**PWP (SDM)**			
Im	RMSE (Best)	RMSE (Wrst)	RMSE (Ave)	RMSE (Std)	RMSE (Best)	RMSE (Wrst)	RMSE (Ave)	RMSE (Std)
W	2.76052E−03	1.54850E−02	7.81464E−03	3.44140E−03	3.43578E−03	2.07530E−02	9.41698E−03	4.43182E−03
G	**7.73006E−04**	7.36945E−02	9.58151E−03	2.41640E−02	2.03999E−03	9.51542E−02	2.81302E−02	4.26587E−02
M	8.39644E−04	1.05243E−01	2.17254E−02	3.46176E−02	2.04495E−03	1.67914E−01	9.37286E−02	5.76032E−02
WM	7.73289E−04	7.40206E−03	3.94523E−03	1.93291E−03	2.15891E−03	7.16408E−03	4.41351E−03	1.57854E−03
GM	7.73006E−04	7.81899E−04	7.73432E−04	1.79852E−06	2.03999E−03	2.04055E−03	2.04003E−03	1.29400E−07
MWG	**7.73006E−04**	**7.73006E−04**	**7.73006E−04**	**2.73165E−17**	**2.03999E−03**	**2.03999E−03**	**2.03999E−03**	**2.55732E−17**
MWGG	**7.73006E−04**	7.75378E−04	7.73101E−04	4.74377E−07	2.03999E−03	3.63447E−03	2.20995E−03	3.41592E−04
	Ultra (SDM)				**STM (SDM)**			
Im	RMSE (Best)	RMSE (Wrst)	RMSE (Ave)	RMSE (Std)	RMSE (Best)	RMSE (Wrst)	RMSE (Ave)	RMSE (Std)
W	1.28403E−02	1.93060E−01	1.09133E−01	5.74690E−02	2.40293E−03	2.07183E−02	8.92497E−03	4.37221E−03
G	2.55107E−03	1.23148E−01	1.18324E−01	2.41195E−02	1.72192E−03	7.94295E−02	1.72634E−02	3.17240E−02
M	8.19443E−03	2.40087E−01	1.58225E−01	4.30057E−02	3.26345E−03	1.46961E−01	4.87871E−02	5.10106E−02
WM	6.38186E−03	1.28938E−01	6.29386E−02	4.93280E−02	1.91973E−03	1.10747E−01	8.73960E−03	2.14608E−02
GM	2.55107E−03	1.23148E−01	7.97333E−02	5.90804E−02	1.72192E−03	1.72192E−03	1.72192E−03	3.86733E−18
MWG	2.55107E−03	1.23148E−01	7.00855E−02	6.10973E−02	**1.72192E−03**	**1.72192E−03**	**1.72192E−03**	**1.86774E−17**
MWGG	**2.55107E−03**	**1.23148E−01**	**7.40209E−03**	**2.41140E−02**	1.72192E−03	1.72192E−03	1.72192E−03	4.52521E−11
	RTC France (DDM)				**PWP (DDM)**			
Im	RMSE (Best)	RMSE (Wrst)	RMSE (Ave)	RMSE (Std)	RMSE (Best)	RMSE (Wrst)	RMSE (Ave)	RMSE (Std)
W	1.97089E−03	1.27830E−02	5.94556E−03	2.95450E−03	2.22875E−03	1.26437E−01	2.26931E−02	3.45255E−02
G	7.32648E−04	6.94424E−02	3.02631E−03	1.25440E−02	2.03999E−03	9.39027E−02	5.34902E−02	4.65317E−02
M	1.07863E−03	1.11716E−01	2.06786E−02	3.43795E−02	2.11217E−03	1.33642E−01	8.15665E−02	5.02481E−02
WM	8.95104E−04	5.88891E−03	2.99333E−03	1.30379E−03	2.14703E−03	9.64258E−02	1.08351E−02	2.56478E−02
GM	7.32649E−04	7.68045E−04	7.41568E−04	9.40324E−06	2.03999E−03	9.39027E−02	5.71760E−03	1.83719E−02
MWG	7.32648E−04	7.72697E−04	7.41190E−04	1.01319E−05	2.03999E−03	9.39027E−02	9.39203E−03	2.54347E−02
MWGG	7.33598E−04	7.73101E−04	7.57319E−04	1.08944E−05	**2.03999E−03**	**2.08064E−03**	**2.04856E−03**	**1.28243E−05**
	Ultra (DDM)				**STM (DDM)**			
Im	RMSE (Best)	RMSE (Wrst)	RMSE (Ave)	RMSE (Std)	RMSE (Best)	RMSE (Wrst)	RMSE (Ave)	RMSE (Std)
W	3.12922E−02	1.55337E−01	1.20179E−01	2.87265E−02	2.33108E−03	2.29162E−02	9.73174E−03	4.45959E−03
G	9.72619E−03	9.52147E−02	8.86639E−02	2.26968E−02	1.68320E−03	7.48355E−02	1.63277E−02	2.98572E−02
M	1.12263E−02	2.44632E−01	1.43575E−01	4.15869E−02	2.14657E−03	1.47807E−01	5.78438E−02	5.88235E−02
WM	9.19250E−03	1.71675E−01	1.02816E−01	4.30575E−02	2.01969E−03	1.51555E−02	5.50998E−03	2.91319E−03
GM	2.57273E−03	9.52147E−02	9.15090E−02	1.85284E−02	1.67763E−03	7.48355E−02	4.61996E−03	1.46283E−02
MWG	**2.57273E−03**	9.52147E−02	8.40978E−02	3.07254E−02	**1.67466E−03**	7.48355E−02	4.61855E−03	1.46285E−02
MWGG	2.57438E−03	**7.52394E−03**	**4.23951E−03**	**1.71379E−03**	**1.67518E−03**	**1.72184E−03**	**1.70641E−03**	**1.44552E−05**

Table 4
Results for SDM-based RTC France.

Algorithms	I_{ph} (A)	I_{sd} (μA)	R_s (Ω)	R_{sh} (Ω)	n	*RMSE (Best)*	*RMSE (Wrst)*	*RMSE (Ave)*	*RMSE (Std)*	*Rank*	*p-value*
SCA	0.7694	1.212E−07	0.0433	25.6595	1.3910	7.62013E−03	2.05864E−02	1.82937E−02	4.05648E−03	10	**1.42E−09**
GNDO	**0.7608**	**3.107E−07**	**0.0365**	**52.8898**	**1.4773**	**7.73006E−04**	7.36945E−02	1.53573E−02	2.97701E−02	7	1.09E−01
AVOA	0.7608	9.367E−08	0.0416	39.3045	1.3660	1.95099E−03	7.36945E−02	1.15509E−02	1.88117E−02	6	**1.42E−09**
EO	0.7608	3.121E−07	0.0365	53.0301	1.4777	7.73041E−04	3.52357E−03	1.57119E−03	5.70870E−04	9	**1.42E−09**
WOA	0.7614	4.449E−07	0.0348	51.3654	1.5144	1.08999E−03	7.85834E−02	3.02193E−02	3.01687E−02	11	**1.42E−09**
GTO	**0.7608**	**3.107E−07**	**0.0365**	**52.8898**	**1.4773**	**7.73006E−04**	1.30874E−03	8.76457E−04	1.25433E−04	3	**1.42E−09**
MPA	0.7611	3.541E−07	0.0359	50.7550	1.4906	8.49454E−04	6.54420E−03	5.19903E−03	1.22850E−03	4	**1.42E−09**
ISA	0.7608	3.126E−07	0.0365	52.8187	1.4779	7.73196E−04	7.36945E−02	1.54488E−02	2.97238E−02	8	**1.41E−09**
GWO	0.7632	4.030E−07	0.0346	33.7379	1.5046	2.10013E−03	7.36946E−02	1.14429E−02	1.37396E−02	5	**1.42E−09**
MWG[a]	**0.7608**	**3.107E−07**	**0.0365**	**52.8898**	**1.4773**	**7.73006E−04**	**7.73006E−04**	**7.73006E−04**	**2.13225E−17**	**1**	
MWGG[a]	**0.7608**	**3.107E−07**	**0.0365**	**52.8898**	**1.4773**	**7.73006E−04**	7.75378E−04	7.73101E−04	4.74377E−07	2	5.05E−01

[a]**Bold** Values mark the best findings.

the best-obtained parameters. In addition, this table compares the outcomes of the proposed algorithm: MWG with these of the others to determine if there is a difference between them based on the Wilcoxon rank-sum test which returns the *p*-value which indicates that there is a difference in a case it is less than 5%; otherwise there is no difference. The column rank is presented in Table 4 and depicted in Fig. 7 shows the order of various algorithms in terms of reaching better Ave. Inspecting this table shows that MWG comes in the 1st rank for the majority of statistical information like best, Ave, worst, and SD, while its outcomes are not significantly different compared to these of GNDO and MWGG because the *p*-value with these algorithms is greater than 5%.

B. **Photowatt-PWP201 module**

This section employs a common PV module known as Photowatt-PWP201 to evaluate the performance of the proposed algorithms. Herein, algorithms are also run 30 times and their results are analyzed to extract the following statistical information: Best, Worst, Ave, and SD. The Wilcoxon rank-sum test, which returns a *p*-value indicating whether there is a difference between the proposed algorithm: MWG, and those of the others, is also used to compare the results of the two algorithms to see if there is a difference. Table 5 and Fig. 8 show that the performance of the proposed algorithms is competitive with each other and superior to all the rival algorithms in this module. For all statistical information like best, worst, Ave, and SD, MWG is

Table 5
Results for SDM-based PWP201 module.

Algorithms	I_{ph} (A)	I_{sd} (μA)	R_s (Ω)	R_{sh} (Ω)	n	*RMSE (Best)*	*RMSE (Wrst)*	*RMSE (Ave)*	*RMSE (Std)*	*Rank*	*p-value*
SCA	1.0282	7.981E−07	0.0407	21.5902	1.2094	7.55526E−03	9.51658E−02	2.64638E−02	2.22379E−02	4	**1.41E−09**
GNDO	1.0324	2.497E−06	0.0345	20.7867	1.3166	2.03999E−03	9.51542E−02	4.30102E−02	4.71738E−02	7	8.07E−02
AVOA	1.0298	1.435E−05	0.0279	99.9997	1.5216	4.67600E−03	9.51542E−02	6.33571E−02	4.32776E−02	9	**1.41E−09**
EO	1.0328	2.339E−06	0.0346	19.6386	1.3101	2.04711E−03	3.32488E−03	2.74044E−03	3.83062E−04	2	**1.41E−09**
WOA	1.0313	5.012E−06	0.0320	29.3974	1.3914	2.58157E−03	9.52555E−02	4.22565E−02	4.26883E−02	6	**1.41E−09**
GTO	1.0324	2.497E−06	0.0345	20.7867	1.3166	2.03999E−03	9.51542E−02	3.19146E−02	4.42772E−02	5	**1.30E−09**
MPA	1.0278	5.938E−06	0.0318	70.9666	1.4103	2.95055E−03	5.84544E−03	4.60701E−03	8.53652E−04	3	**1.41E−09**
ISA	1.0323	2.514E−06	0.0344	20.8787	1.3173	2.04005E−03	9.51542E−02	5.79155E−02	4.65484E−02	8	**9.23E−10**
GWO	1.0382	6.276E−07	0.0384	11.1023	1.1903	3.57253E−03	9.51542E−02	6.36929E−02	4.28393E−02	10	**1.41E−09**
MWG[a]	**1.0324**	**2.497E−06**	**0.0345**	**20.7867**	**1.3166**	**2.03999E−03**	**2.03999E−03**	**2.03999E−03**	**9.64188E−18**	**1**	
MWGG[a]	**1.0324**	**2.497E−06**	**0.0345**	**20.7868**	**1.3166**	**2.03999E−03**	**2.03999E−03**	**2.03999E−03**	3.81708E−12	**1**	1.70E−01

[a]**Bold** Values mark the best findings.

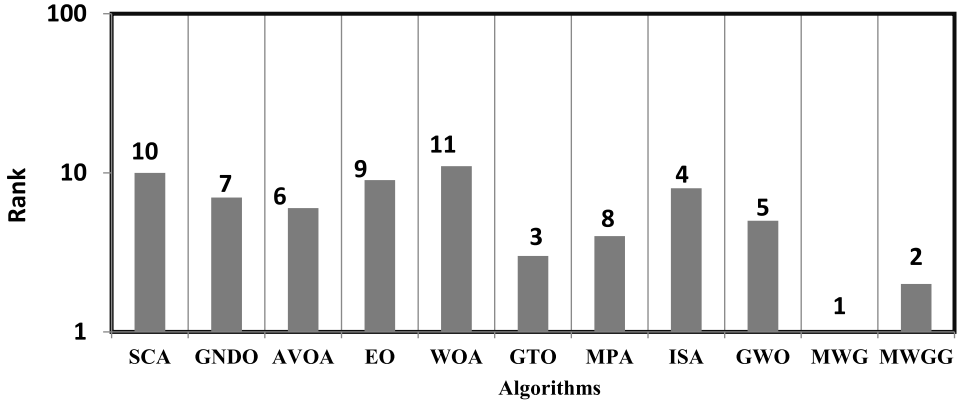

Fig. 7. Depiction of Rank of each algorithm over SDM-based RTC France.

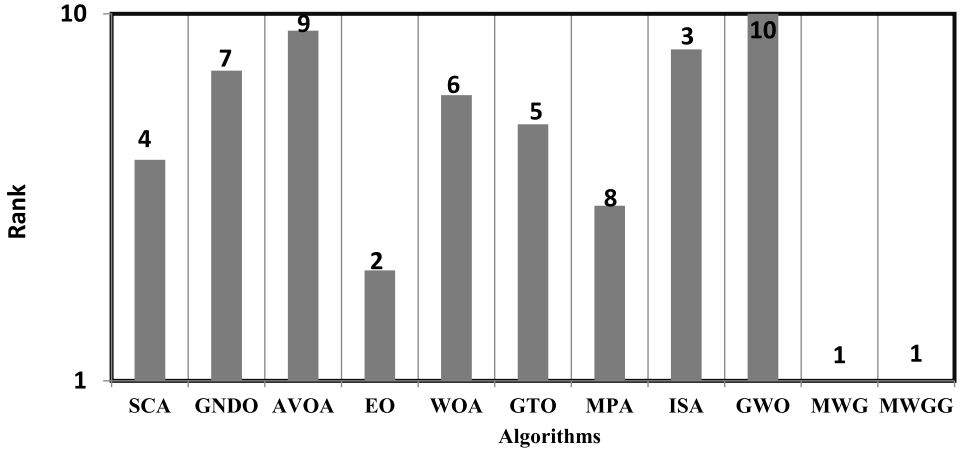

Fig. 8. Depiction of Rank of each algorithm over SDM-based PWP201 module.

ranked 1st according to this table, while MWGG is ranked 2nd for SD.

C. **Ultra 85-P module**

For the purposes of further evaluating the performance of the proposed algorithms, a common photovoltaic module known as Ultra 85-P is used in this section. A total of 30 runs for each algorithm are performed and the results are analyzed to obtain the following statistical information: best, worst, average, and standard deviation (SD). Additionally, the Wilcoxon rank-sum test, which provides an indication of whether there is a difference between the proposed algorithm: MWG, and the results of the other algorithms, is used to compare the results of each pair of algorithms in order to determine whether there is a difference. Table 6 and Fig. 9 demonstrate that the performance of MWGG is superior to the performance of all other competing algorithms over this particular module. MWG is ranked first for all statistical information such as best, worst, Ave, *p*-value, and SD, according to the data in this table.

D. **STM6-40 module**

This section makes use of another common photovoltaic module known as the STM6-40 in order to evaluate the performance of the proposed algorithms in greater depth. It is necessary to perform a total of 30 runs for each algorithm, and the results must be analyzed in order to obtain the following statistical information: the best, worst, average, and standard deviation (SD). A second test, the Wilcoxon rank-sum test, is used to determine

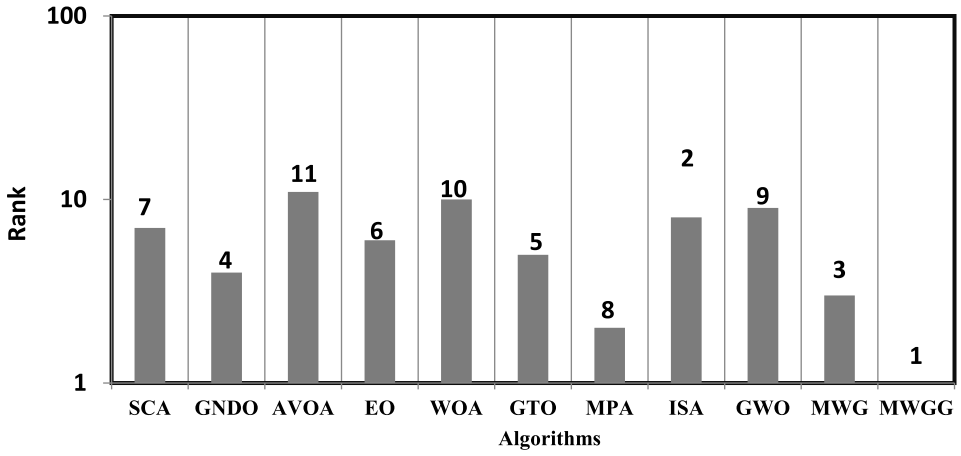

Fig. 9. Depiction of Rank of each algorithm over SDM-based Ultra module.

Table 6
Results for SDM-based Ultra module.

Algorithms	I_{ph} (A)	I_{sd} (μA)	R_s (Ω)	R_{sh} (Ω)	n	*RMSE (Best)*	*RMSE (Wrst)*	*RMSE (Ave)*	*RMSE (Std)*	*Rank*	*p-value*
SCA	5.2165	2.754E−07	0.0139	3.0113	1.2268	4.22246E−02	1.59703E−01	1.00069E−01	3.70740E−02	7	**5.20E−03**
GNDO	**5.2271**	**1.043E−05**	**0.0110**	**3.7997**	**1.5682**	**2.55107E−03**	1.23148E−01	7.09708E−02	6.01421E−02	4	**2.21E−03**
AVOA	5.7225	1.671E−07	0.2470	100.00	1.3590	1.23148E−01	1.70300E−01	1.37452E−01	1.56267E−02	11	**1.41E−09**
EO	5.2267	1.065E−05	0.0110	3.8311	1.5707	2.55668E−03	1.23403E−01	9.05371E−02	5.34379E−02	6	**3.29E−05**
WOA	5.2621	7.979E−06	0.0111	2.5284	1.5376	9.32387E−03	2.85569E−01	1.19709E−01	6.00890E−02	10	**9.69E−06**
GTO	**5.2271**	**1.043E−05**	**0.0110**	**3.7997**	**1.5682**	**2.55107E−03**	1.23148E−01	7.10953E−02	5.99906E−02	5	**8.94E−03**
MPA	5.2067	3.044E−05	0.0100	7.1106	1.7059	9.39523E−03	3.10305E−02	1.59876E−02	4.56796E−03	2	**4.73E−03**
ISA	5.1683	2.464E−05	0.0104	50.162	1.6761	1.43296E−02	1.72373E−01	1.18854E−01	4.18732E−02	8	**2.91E−06**
GWO	5.1634	2.533E−06	0.0129	11.334	1.4166	2.75297E−02	1.23868E−01	1.19523E−01	1.91662E−02	9	**7.37E−09**
MWG[a]	**5.2271**	**1.043E−05**	**0.0110**	**3.7997**	**1.5682**	**2.55107E−03**	1.23148E−01	7.00855E−02	6.10973E−02	3	**1.70E−03**
MWGG[a]	**5.2271**	**1.043E−05**	**0.0110**	**3.7997**	**1.5682**	**2.55107E−03**	**4.34533E−03**	**2.64859E−03**	**3.68608E−04**	**1**	

[a]**Bold** Values mark the best findings.

Table 7
Results for SDM-based STM module.

Algorithms	I_{ph} (A)	I_{sd} (μA)	R_s (Ω)	R_{sh} (Ω)	n	*RMSE (Best)*	*RMSE (Wrst)*	*RMSE (Ave)*	*RMSE (Std)*	*Rank*	*p-value*
SCA	1.6557	7.961E−06	0.0000	70.5150	1.7079	5.40425E−03	2.46926E−02	1.26618E−02	4.05560E−03	7	**2.56E−08**
GNDO	**1.6639**	**1.741E−06**	**0.0043**	**15.9315**	**1.5205**	**1.72192E−03**	5.55232E−03	1.93943E−03	8.18352E−04	3	**1.97E−03**
AVOA	1.6602	3.933E−06	0.0016	25.1500	1.6155	2.70184E−03	7.94295E−02	1.46419E−02	1.99678E−02	8	**2.05E−08**
EO	1.6620	2.496E−06	0.0032	19.4279	1.5610	1.98129E−03	7.94295E−02	5.93556E−03	1.53173E−02	6	**2.29E−08**
WOA	1.6642	5.860E−06	0.0000	20.7612	1.6670	3.72099E−03	6.71027E−02	2.48795E−02	1.99900E−02	10	**2.56E−08**
GTO	**1.6639**	**1.741E−06**	**0.0043**	**15.9334**	**1.5205**	**1.72192E−03**	4.29114E−03	2.62055E−03	8.90810E−04	4	**2.56E−08**
MPA	1.6613	4.065E−06	0.0017	24.2064	1.6197	2.77803E−03	5.55537E−03	4.26425E−03	7.19416E−04	2	**2.56E−08**
ISA	1.6638	1.794E−06	0.0042	16.0823	1.5238	1.72332E−03	7.94295E−02	2.66044E−02	3.69850E−02	11	**1.10E−08**
GWO	1.6636	5.541E−06	0.0000	20.4707	1.6596	3.48792E−03	7.94300E−02	1.86996E−02	1.88769E−02	9	**2.05E−08**
MWG[a]	**1.6639**	**1.741E−06**	**0.0043**	**15.9315**	**1.5205**	**1.72192E−03**	7.94295E−02	4.83023E−03	1.55415E−02	5	**1.70E−08**
MWGG[a]	**1.6639**	**1.741E−06**	**0.0043**	**15.9315**	**1.5205**	**1.72192E−03**	**1.73095E−03**	**1.72228E−03**	**1.80604E−06**	**1**	

[a]**Bold** Values mark the best findings.

whether there is a difference between the results of the proposed algorithm: MWGG, and the results of the other algorithms. Table 7 and Fig. 10 demonstrate that the performance of MWGG is superior to the performance of all other competing algorithms over this particular module. Whereas, in accordance with the data in this table, MWGG is ranked first for all statistical information, including the best and worst, the average (Ave), the *p*-value, and the SD.

5.2.2. Qualitative analysis

This section compares the proposed algorithms with the other competing algorithms in terms of the convergence curve and boxplot to elaborate their ability for reaching the near-optimal solution through less number of function evaluations in addition to the quality of their outcomes according to the five-number summary (maximum, median, minimum, first quartile and third quartile). Furthermore, this section depicts the I–V curve between measured and estimated data to show how far the estimated parameters could reach the current which is consistent with the measured.

A. **Convergence curve**

This section discusses the convergence curve which is depicted in Fig. 11. According to this figure, the proposed algorithm GMW could reach the near-optimal solution faster than all the rival algorithms for RTC France solar cell and PWP module, followed by GMWG as the second faster one. For the other two test cases: ultra and stem modules, GMWG has a higher speed than all the others. Finally, it is concluded that GMWG could be faster than all rival algorithms for all the test cases; however, for some test cases like RTC France solar cell, and PWP module, GMW is better.

B. **Boxplot (Five-summary number)**

To further demonstrate the superiority of the proposed algorithms, Fig. 12 is presented to represent the five-number summary graphically according to the boxplot for the given set of

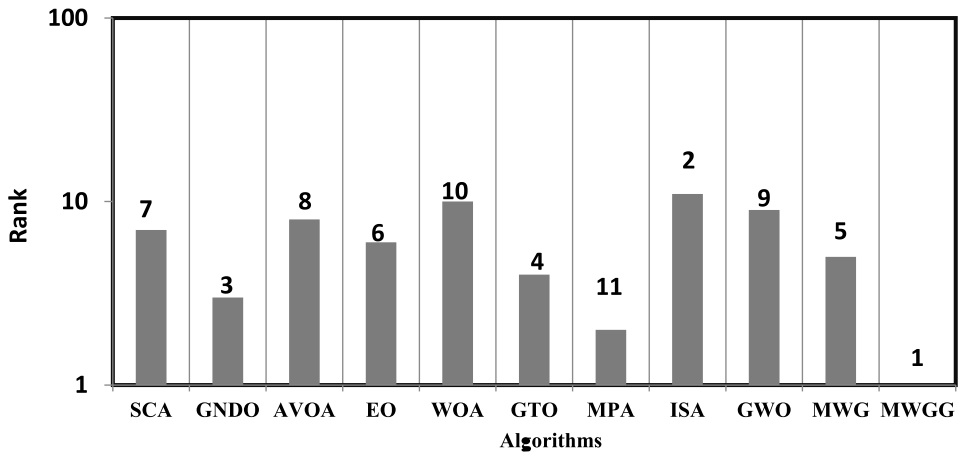

Fig. 10. Depiction of Rank of each algorithm over SDM-based STM module.

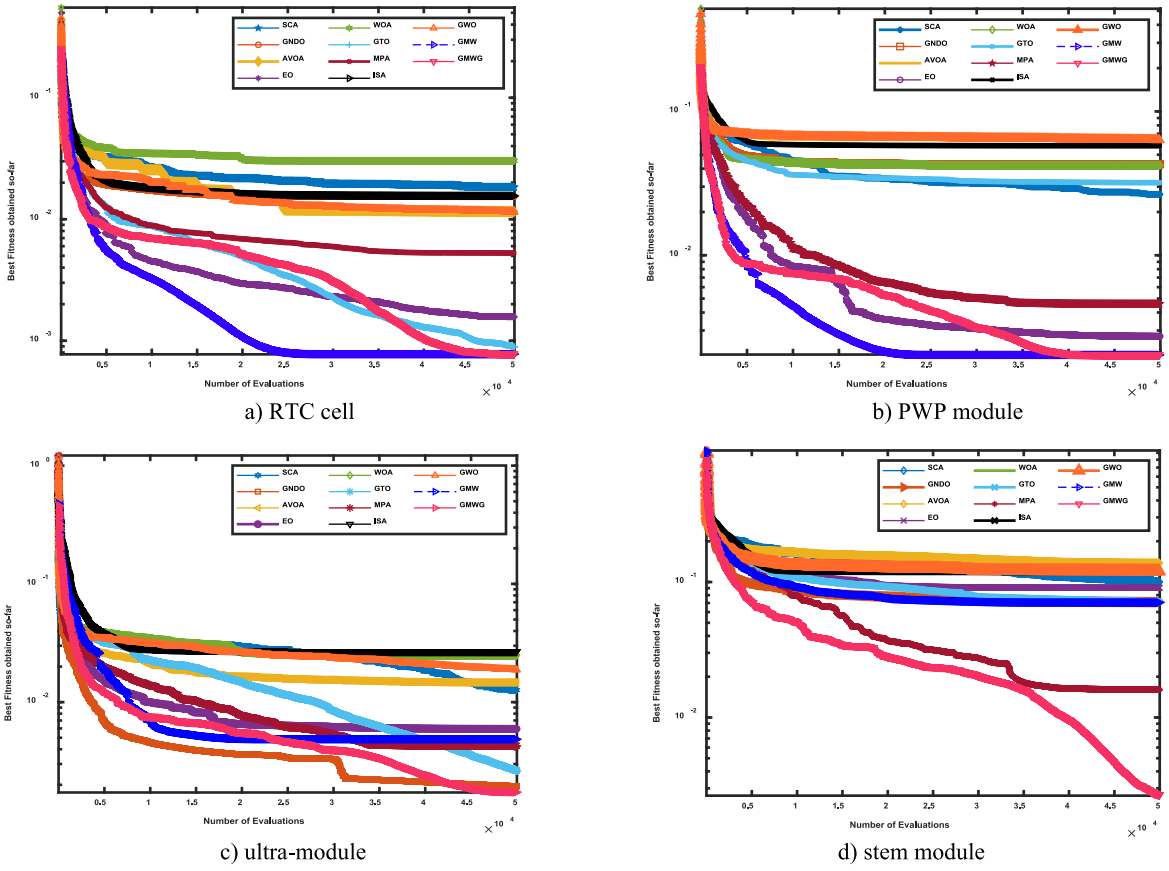

Fig. 11. Depiction of convergence curve of each algorithm over various observed test cases.

findings; this five-number summary represents the maximum, minimum, median, first quartile, and third quartile for the given set of findings. It can be seen in this figure that the performance of the two-proposed algorithms is so similar for RTC France solar cell and PWP module, but for the other test cases, GMMG could be the most appropriate for the five-number summary.

C. **Quality analysis**

This section compares the difference between the I–V curve generated according to the measured data and this estimated by the GMWG as shown in Fig. 13 for various observed test cases, which shows that the GMWG picks parameter values that make simulated data that is very close to the real data. Finally, in Fig. 14, you can see the difference between the measured and estimated current.

5.3. Comparison over double-diode model (DDM)

Like SDM discussed in the previous section, this section shows how the proposed algorithms and other algorithms did when they tried to solve the DDM over a variety of PV modules and a cell from RTC France. In this section, we do two things: First, we look at the algorithms' performance in terms of the best,

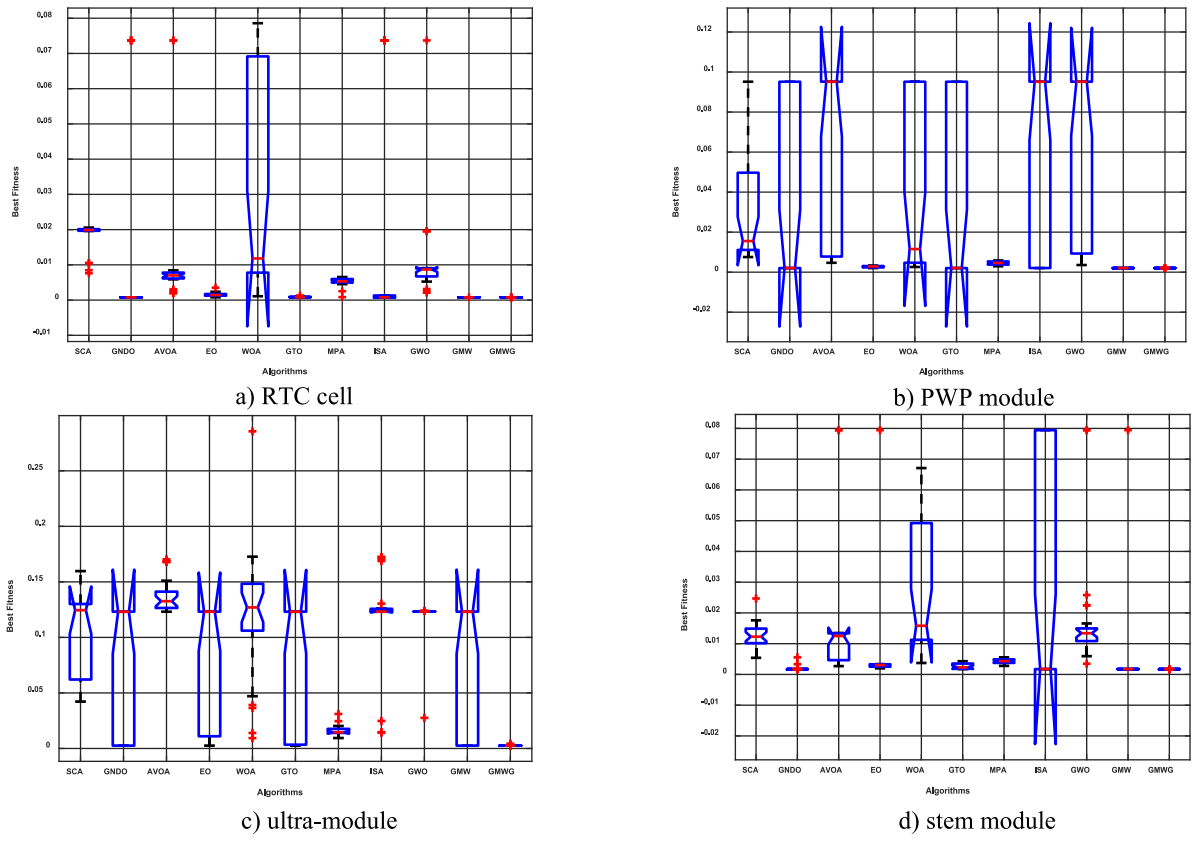

Fig. 12. Depiction of Boxplot of algorithms over various observed test cases.

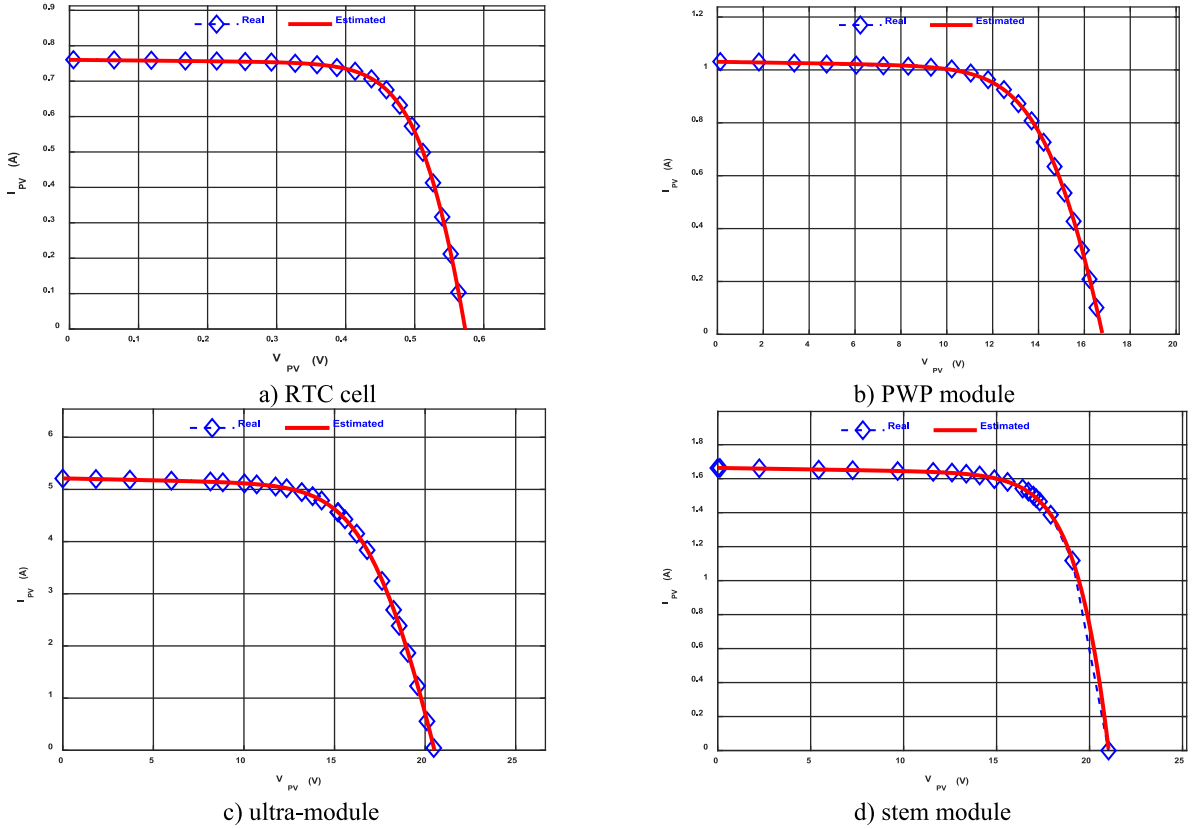

Fig. 13. Depiction of I–V characteristics curves according to the parameters estimated by GMWG.

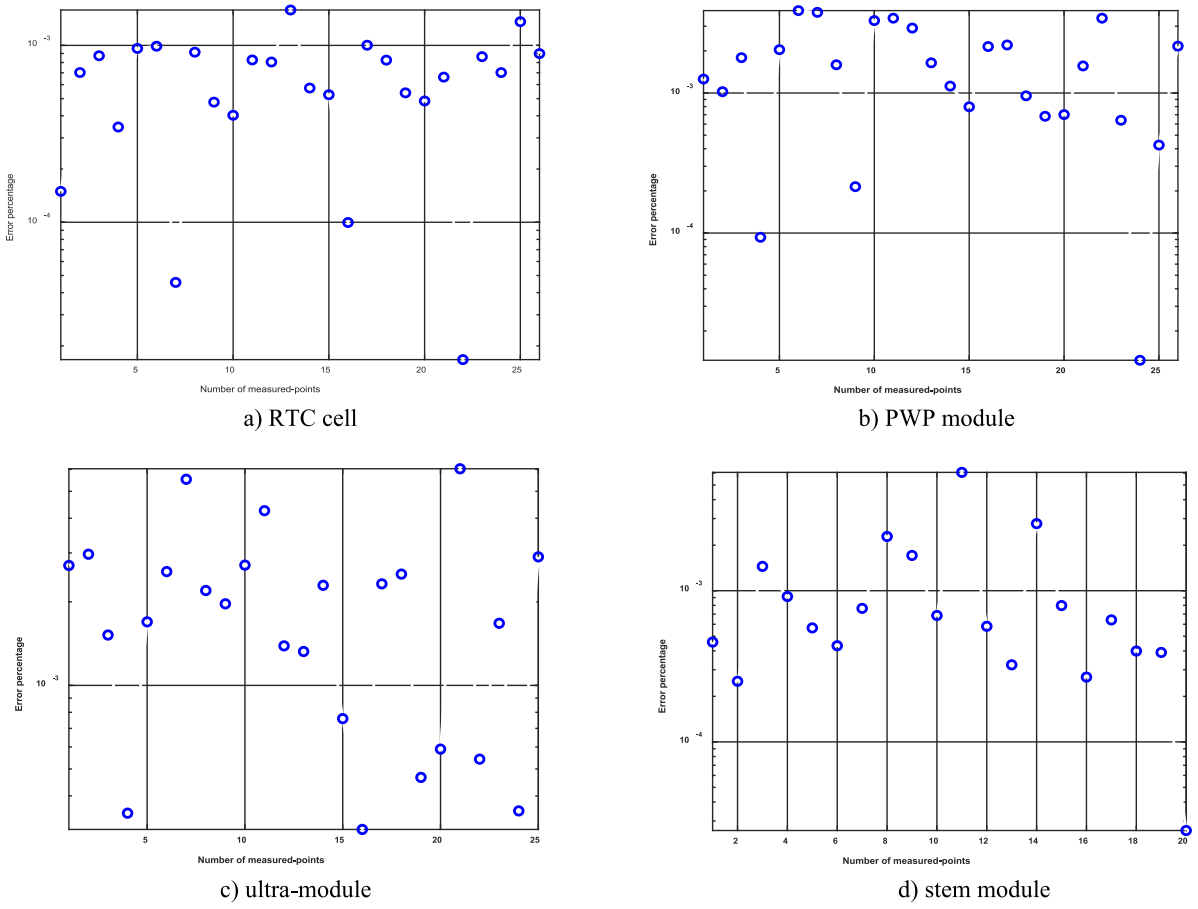

Fig. 14. Depiction of difference between the measured current and current estimated using GMWG.

average, worst, and standard deviation of RMSE values, as well as the *p*-value of the Wilcoxon rank-sum test, to see if there is a difference between the proposed algorithms and those of the rival optimizers. Second, we look at the algorithms' visual performance by comparing them to each other.

5.3.1. Quantitative analysis

Quantitative analysis is the first step in this section and it compares the proposed algorithms with those of rival optimizers for three PV modules and a solar cell using statistical information (Best, Ave, Worst, *p*-value, SD).

A. **R.T.C France**

For this case, it is necessary to run each algorithm 30 times to obtain the following statistical data: best, average, worst, and standard deviation (SD), all of which can be found in Table 7 along with the best-obtained parameters. To determine if there is a significant difference between the proposed algorithm: MWG and other algorithms, the Wilcoxon rank-sum test is used to calculate a *p*-value that indicates that there is a difference whether this value is 5%; otherwise there is no difference. Table 8 and Fig. 15 show the ranking of algorithms in terms of their ability to achieve a better average. In this table, MWG ranks first for the majority of statistical information, including best, worst, and SD, but its results are not significantly different from those of MWGG because p-values with this algorithm are greater than 5%.

B. **Photowatt-PWP201 module**

Another common PV module, Photowatt-PWP201, is used in this section to further evaluate the performance of the algorithms proposed. As a result of executing each algorithm 30 independent times, the following statistical information is extracted: Best/Worst/Average/SD and showed in Table 9. Also, this table includes the *p*-value of Wilcoxon rank-sum test used to compare the results of the two algorithms to see if there is a difference between those of MWG and those of the others. According to the results in Table 9 and Fig. 16, MWGG outperform all other algorithms for this module. MWGG tops the table for every type of statistic, including best, worst, average, and standard deviation, while MWG comes in fifth rank after GTO, MPA, and AVOA.

C. **Ultra 85-P module**

This section uses a common photovoltaic module known as Ultra 85-P to further evaluate the performance of the proposed algorithms. In order to obtain the statistical information, a total of 30 runs for algorithms are carried out and the results are analyzed. Wilcoxon rank-sum test, which indicates whether, the proposed algorithm: MWG differs from those of other algorithms, has been used to compare the results of both algorithms in order to determine that there are differences between them. All other competing algorithms' performance over this particular module is shown to be inferior to MWGG's performance according to Table 10 and Fig. 17. According to the data in this table, MWG ranks first for the following statistical information, including best, Ave, and *p*-value.

D. **STM6-40 module**

The STM6-40 photovoltaic module is used in this section to examine the proposed algorithms' performance in greater depth. All algorithms are run 30 independent times and the results are analyzed to obtain the following statistical data: best, worst,

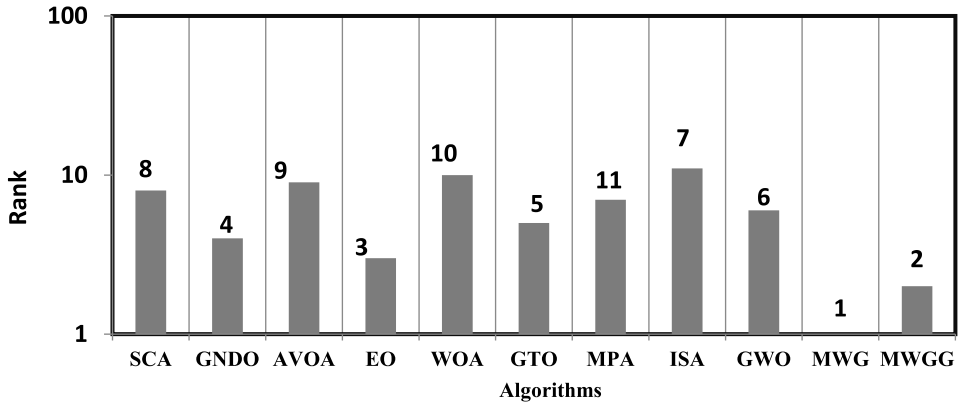

Fig. 15. Depiction of Rank of each algorithm over DDM-based RTC France.

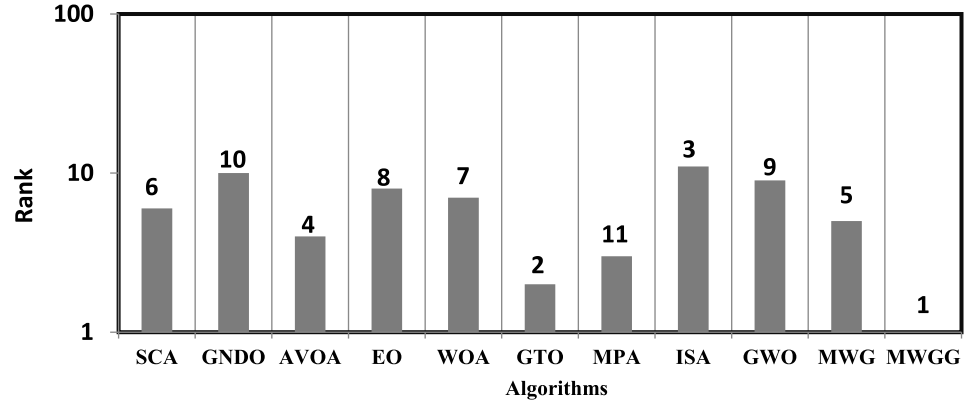

Fig. 16. Depiction of Rank of each algorithm over DDM-based PWP201 module.

Table 8
Results for DDM-based RTC France.

Algorithms	I_{ph} (A)	I_{sd1} (μA)	I_{sd2} (μA)	R_s (Ω)	R_{sh} (Ω)	n_1	n_2	*RMSE (Best)*	*RMSE (Wrst)*	*RMSE (Ave)*	*RMSE (Std)*	*Rank*	*p-value*
SCA	0.759	1.17E−08	1.77E−06	0.039	264.345	1.264	1.758	4.534E−03	2.485E−02	1.152E−02	5.420E−03	8	**1.42E−09**
GNDO	0.761	8.66E−08	2.16E−06	0.038	58.356	1.373	2.000	7.326E−04	6.944E−02	3.485E−03	1.374E−02	4	**1.23E−02**
AVOA	0.761	2.08E−07	2.24E−07	0.037	51.679	1.444	1.784	7.889E−04	6.944E−02	1.188E−02	2.177E−02	9	**1.42E−09**
EO	0.761	1.20E−07	1.04E−06	0.037	60.653	1.405	1.849	7.713E−04	3.317E−03	1.692E−03	6.273E−04	3	**1.42E−09**
WOA	0.758	1.13E−09	4.64E−07	0.036	285.590	1.342	1.520	2.070E−03	7.037E−02	1.697E−02	2.168E−02	10	**1.42E−09**
GTO	0.761	9.88E−08	1.98E−06	0.038	57.813	1.383	2.000	7.331E−04	6.944E−02	3.827E−03	1.368E−02	5	**6.57E−09**
MPA	0.759	1.06E−09	6.31E−07	0.034	170.088	1.504	1.552	1.743E−03	1.523E−02	6.097E−03	3.483E−03	7	**1.42E−09**
ISA	0.761	1.97E−07	9.27E−07	0.037	55.478	1.439	2.000	7.497E−04	6.944E−02	2.282E−02	3.264E−02	11	**1.52E−09**
GWO	0.761	3.90E−09	4.96E−06	0.042	74.898	1.163	2.000	1.196E−03	2.675E−02	5.915E−03	6.093E−03	6	**1.42E−09**
MWG[a]	**0.761**	**8.66E−08**	**2.16E−06**	**0.038**	**58.356**	**1.373**	**2.000**	**7.326E−04**	**7.502E−04**	**7.348E−04**	**4.395E−06**	**1**	
MWGG[a]	0.761	1.27E−07	1.62E−06	0.038	56.779	1.403	1.999	7.365E−04	7.727E−04	7.538E−04	1.005E−05	2	2.01E−01

[a]**Bold** Values mark the best findings.

Table 9
Results for DDM-based PWP201 module.

Algorithms	I_{ph} (A)	I_{sd1} (μA)	I_{sd2} (μA)	R_s (Ω)	R_{sh} (Ω)	n_1	n_2	*RMSE (Best)*	*RMSE (Wrst)*	*RMSE (Ave)*	*RMSE (Std)*	*Rank*	*p-value*
SCA	1.031	2.23E−09	1.92E−06	0.038	121.799	1.000	1.294	6.986E−03	1.827E−02	1.291E−02	3.199E−03	6	**1.42E−09**
GNDO	1.032	1.38E−09	2.50E−06	0.034	20.787	1.317	1.317	2.040E−03	9.390E−02	7.186E−02	4.004E−02	10	**1.00E−06**
AVOA	1.030	1.28E−09	4.85E−06	0.032	32.956	1.241	1.388	2.515E−03	9.390E−02	8.011E−03	1.795E−02	4	**1.42E−09**
EO	1.032	1.95E−06	1.95E−06	0.035	21.308	1.297	1.681	2.078E−03	9.390E−02	3.159E−02	4.363E−02	8	**1.60E−09**
WOA	1.036	1.01E−09	6.93E−07	0.038	13.088	1.008	1.200	3.331E−03	9.430E−02	3.096E−02	3.696E−02	7	**1.42E−09**
GTO	1.032	1.00E−09	2.50E−06	0.034	20.787	1.316	1.317	2.040E−03	3.385E−03	2.197E−03	3.706E−04	2	**4.78E−02**
MPA	1.031	3.48E−09	6.92E−07	0.039	17.612	1.062	1.200	3.706E−03	1.578E−02	7.705E−03	2.162E−03	3	**1.42E−09**
ISA	1.032	1.15E−07	2.79E−06	0.034	22.302	1.188	1.350	2.072E−03	9.390E−02	8.659E−02	2.532E−02	11	**1.60E−09**
GWO	1.034	2.61E−06	3.64E−06	0.033	18.980	1.327	1.783	2.509E−03	9.393E−02	6.513E−02	4.195E−02	9	**1.42E−09**
MWG[a]	1.032	1.03E−09	2.50E−06	0.034	20.787	1.317	1.317	2.040E−03	9.390E−02	9.392E−03	2.543E−02	**5**	**8.86E−05**
MWGG[a]	**1.032**	**6.95E−07**	**1.80E−06**	**0.034**	**20.787**	**1.317**	**1.317**	**2.040E−03**	**2.081E−03**	**2.049E−03**	**1.264E−05**	**1**	

[a]**Bold** Values mark the best findings.

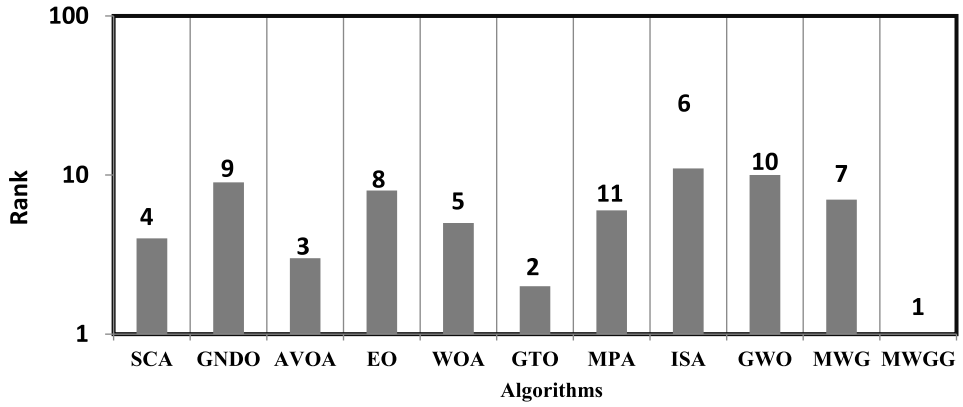

Fig. 17. Depiction of Rank of each algorithm over DDM-based Ultra module.

Table 10
Results for DDM-based Ultra module.

Algorithms	I_{ph} (A)	I_{sd1} (μA)	I_{sd2} (μA)	R_s (Ω)	R_{sh} (Ω)	n_1	n_2	*RMSE (Best)*	*RMSE (Wrst)*	*RMSE (Ave)*	*RMSE (Std)*	*Rank*	*p-value*
SCA	1.031	2.23E−09	1.92E−06	0.038	121.799	1.000	1.294	2.856E−02	1.252E−01	6.659E−02	3.142E−02	4	**2.30E−08**
GNDO	1.032	1.38E−09	2.50E−06	0.034	20.787	1.317	1.317	9.521E−02	9.521E−02	9.521E−02	4.573E−09	9	**2.56E−08**
AVOA	1.030	1.28E−09	4.85E−06	0.032	32.956	1.241	1.388	1.705E−02	1.196E−01	4.624E−02	2.935E−02	3	**2.57E−08**
EO	1.032	1.95E−06	1.95E−06	0.035	21.308	1.297	1.681	5.445E−02	1.068E−01	9.781E−02	9.621E−03	8	**2.57E−08**
WOA	1.036	1.01E−09	6.93E−07	0.038	13.088	1.008	1.200	3.025E−02	1.623E−01	7.670E−02	3.962E−02	5	**1.84E−08**
GTO	1.032	1.00E−09	2.50E−06	0.034	20.787	1.316	1.317	3.597E−03	9.521E−02	1.382E−02	1.820E−02	2	**5.56E−07**
MPA	1.031	3.48E−09	6.92E−07	0.039	17.612	1.062	1.200	1.612E−02	1.536E−01	7.541E−02	4.273E−02	6	**1.46E−08**
ISA	1.032	1.15E−07	2.79E−06	0.034	22.302	1.188	1.350	9.521E−02	1.450E−01	1.063E−01	1.300E−02	11	**2.29E−08**
GWO	1.034	2.61E−06	3.64E−06	0.033	18.980	1.327	1.783	3.511E−02	1.485E−01	1.039E−01	2.888E−02	10	**1.31E−08**
MWG[a]	1.032	1.03E−09	2.50E−06	0.034	20.787	1.317	1.317	**2.573E−03**	**9.521E−02**	8.780E−02	2.565E−02	7	**3.50E−06**
MWGG[a]	**1.032**	**6.95E−07**	**1.80E−06**	**0.034**	**20.787**	**1.317**	**1.317**	**2.573E−03**	1.231E−01	**8.086E−03**	**2.399E−02**	**1**	

[a]**Bold** Values mark the best findings.

Table 11
Results for DDM-based STM module.

Algorithms	I_{ph} (A)	I_{sd1} (μA)	I_{sd2} (μA)	R_s (Ω)	R_{sh} (Ω)	n_1	n_2	*RMSE (Best)*	*RMSE (Wrst)*	*RMSE (Ave)*	*RMSE (Std)*	*Rank*	*p-value*
SCA	1.656	1.25E−08	4.46E−07	0.011	19.089	1.167	1.447	1.056E−02	2.349E−02	1.597E−02	3.539E−03	7	**1.42E−09**
GNDO	1.664	1.56E−08	4.77E−06	0.007	17.327	1.177	1.733	1.679E−03	7.697E−02	1.645E−02	3.001E−02	8	4.85E−01
AVOA	1.665	1.61E−09	1.44E−06	0.005	14.302	1.496	1.500	1.827E−03	1.250E−02	7.387E−03	3.375E−03	4	**1.42E−09**
EO	1.664	1.38E−07	4.91E−06	0.006	16.604	1.317	1.796	1.692E−03	7.484E−02	2.551E−02	3.455E−02	10	**2.20E−06**
WOA	1.648	1.67E−09	3.70E−06	0.001	173.952	1.593	1.607	8.027E−03	3.557E−02	1.885E−02	7.330E−03	9	**1.42E−09**
GTO	1.664	1.00E−09	3.52E−06	0.008	17.192	1.035	1.660	**1.675E−03**	5.538E−03	1.969E−03	8.262E−04	2	8.16E−01
MPA	1.662	1.40E−06	4.99E−06	0.003	20.350	1.509	2.000	2.047E−03	1.718E−02	7.793E−03	4.118E−03	5	**1.42E−09**
ISA	1.664	6.09E−07	4.23E−06	0.005	16.591	1.430	1.890	1.699E−03	7.484E−02	5.737E−02	3.172E−02	11	**2.55E−08**
GWO	1.657	8.42E−09	4.48E−06	0.002	42.190	1.411	1.633	3.768E−03	1.468E−02	9.588E−03	3.295E−03	6	**1.42E−09**
MWG[a]	1.664	1.00E−09	3.59E−06	0.008	17.268	1.034	1.664	**1.675E−03**	7.484E−02	4.618E−03	1.463E−02	3	**5.87E−03**
MWGG[a]	**1.664**	**2.22E−09**	**3.83E−06**	**0.008**	**17.263**	**1.073**	**1.678**	**1.676E−03**	**1.758E−03**	**1.707E−03**	**1.749E−05**	**1**	

[a]**Bold** Values mark the best findings.

average, and standard deviation (SD). To determine if the proposed algorithm MWG's results differ from those of the other algorithms, the Wilcoxon rank-sum test is used to see if this is true. There is no other algorithm that performs better over this particular module than MWGG, as shown in Table 11 and Fig. 18. According to this table, it is clear that MWGG is at the top of every statistical measure, including best and worst, average (Ave), and standard deviation (SD), with the exception of *p*-value, where MWGG could reach less value when comparing with GNDO and GTO.

5.3.2. Quantitative analysis

Algorithms are compared to each other based on a boxplot and a convergence curve, which show how many function evaluations it takes to get to a near-optimal solution, and how good their results are based on a 5-number scorecard (maximum, median, minimum, first quartile and third quartile). The I–V curve between measured and estimated data is shown here to show how far the estimated parameters can reach the current that is consistent with the measured currents.

A. **Convergence curve**

Fig. 19 depicts the convergence curve discussed here. For RTC France solar cells, GMW is the fastest algorithm, followed by GMWG, which is the second-fastest. GMWG outperforms all rival algorithms for the other test cases (PWP, ultra, and stem modules). Conclusion: GMWG may be faster than all rival algorithms for most test cases, but GMW is better for some test cases like RTC France solar cell.

B. **Boxplot (Five-summary number)**

Additionally, Fig. 20 shows the five-number summary according to a boxplot for a given set of results obtained over various DDM-based test cases; this five-number summary represents the

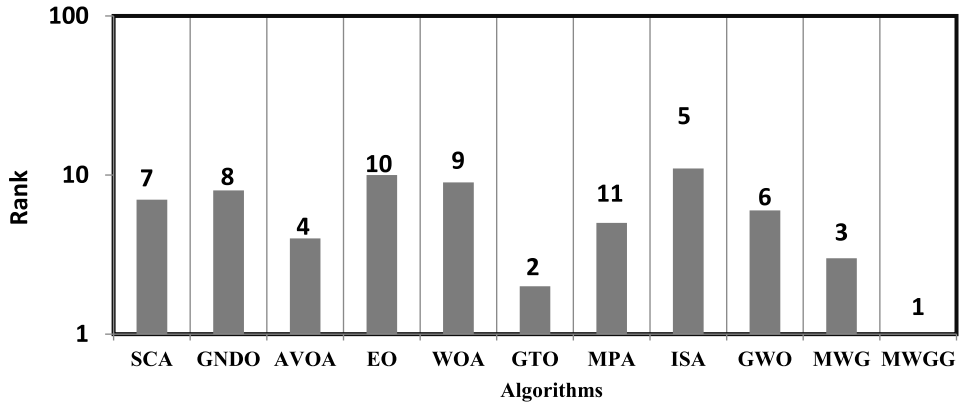

Fig. 18. Depiction of Rank of each algorithm over DDM-based STM module.

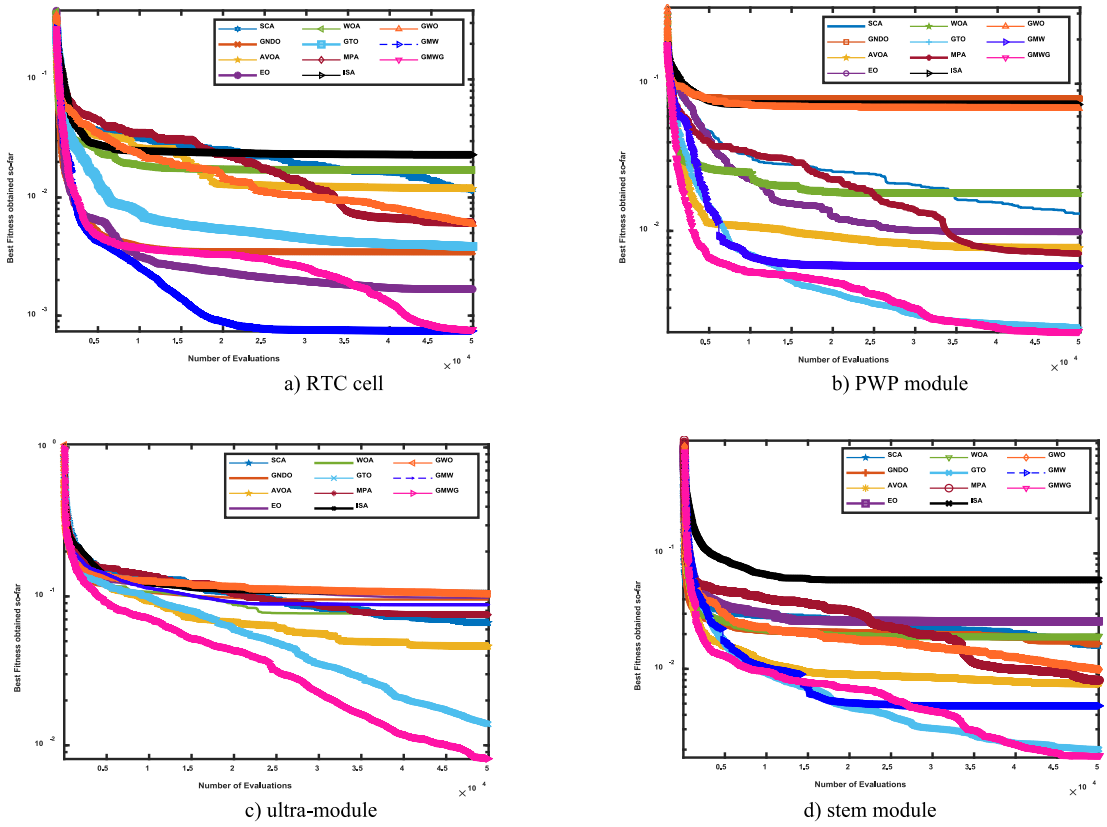

Fig. 19. Depiction of convergence curve of each algorithm over various DDM-based observed test cases.

maximum, minimum, median, first quartile, and third quartile for the given set of results in graphic form to further demonstrate the superiority of the proposed algorithms. For the RTC France solar cell and PWP module, the performance of the two proposed algorithms is very similar, but GMWG may be the most appropriate for the five-number summary in the other test cases.

6. Conclusion

In this paper, a hybrid nature-inspired metaheuristic algorithm is presented for estimating the unknown parameters of SDM and DDM. This hybrid algorithm is based on integrating some updating schemes from three well-known optimization algorithms: WOA, MPA, and GNDO to develop a new stronger variant that is more effective in terms of exploration and exploitation; this variant is referred to as GWM. In addition, this newly proposed variant, GWM, is integrated with two additional optimization methods to further its exploration and exploitation operators' ability to achieve better performance when estimating the unknown parameters of SDM and DDM; This variant is referred to as MWGG. A solar cell from RTC France and three commercial PV module models, including the Photowatt-PWP201 (PWP), Ultra 85-P (Ultra), and STM6-40/36 (STM), are being used to evaluate the proposed algorithm's efficacy and efficiency. The experimental findings demonstrated that MWGG is more accurate and faster at convergent results. Our future work includes

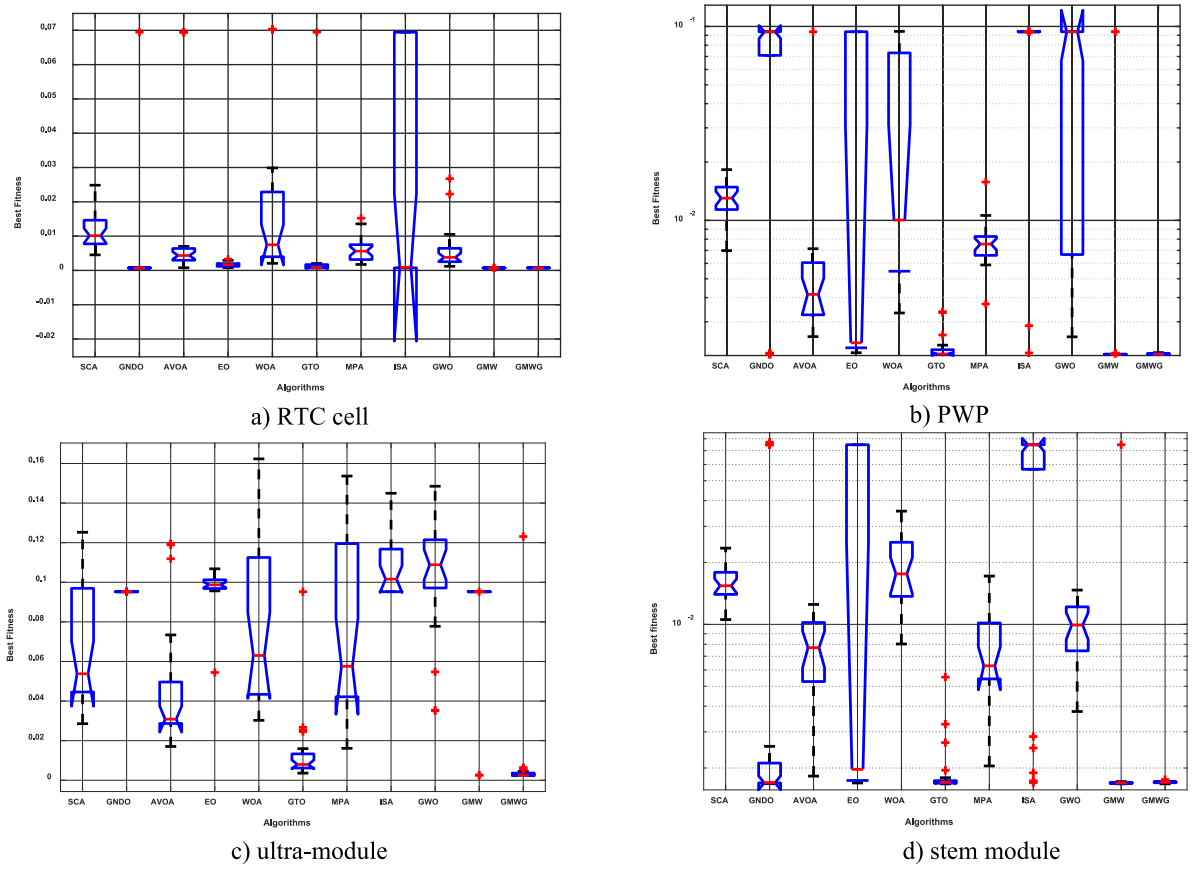

Fig. 20. Depiction of Boxplot of algorithms over various DDM-based observed test cases.

applying the proposed algorithm: MWGG to other optimization problems such as the parameter estimation of a fuel cell, the DNA fragment assembly problem, multi-objective optimization problems, the 0-1 knapsack problem, multidimensional knapsack problem, task scheduling in IoT-based fog computing, and feature selection.

CRediT authorship contribution statement

Mohamed Abdel-Basset: Conceptualization, Methodology, Software, Validation, Formal analysis, Resources, Data curation, Writing – original draft, Writing – review & editing, Visualization, Supervision, Project administration. **Reda Mohamed:** Conceptualization, Methodology, Software, Validation, Formal analysis, Resources, Data curation, Writing – original draft, Writing – review & editing, Visualization, Project administration. **Marwa Sharawi:** Conceptualization, Investigation, Data curation, Visualization, Funding acquisition. **Laila Abdel-Fatah:** Conceptualization, Validation, Writing – review & editing. **Mohamed Abouhawwash:** Methodology, Software, Formal analysis, Investigation, Resources, Data curation, Writing – original draft, Writing – review & editing, Visualization. **Karam Sallam:** Software, Investigation, Writing – review & editing.

Declaration of competing interest

The authors declare that they have no known competing financial interests or personal relationships that could have appeared to influence the work reported in this paper.

Data availability

No data was used for the research described in the article.

Acknowledgments

All authors approved the version of the manuscript to be published.

Funding

There is no funding received for this study.

References

Abd Elaziz, M., Oliva, D., 2018. Parameter estimation of solar cells diode models by an improved opposition-based whale optimization algorithm. Energy Convers. Manage. 171, 1843–1859. http://dx.doi.org/10.1016/J.ENCONMAN.2018.05.062.

Abdel-Basset, M., El-Shahat, D., Chakrabortty, R.K., Ryan, M., 2021a. Parameter estimation of photovoltaic models using an improved marine predators algorithm. Energy Convers. Manage. 227, 113491. http://dx.doi.org/10.1016/J.ENCONMAN.2020.113491.

Abdel-Basset, M., Mohamed, R., Mirjalili, S., Chakrabortty, R.K., Ryan, M.J., 2020. Solar photovoltaic parameter estimation using an improved equilibrium optimizer. Sol. Energy 209, 694–708. http://dx.doi.org/10.1016/J.SOLENER.2020.09.032.

Abdel-Basset, M., et al., 2021b. Parameters identification of PV triple-diode model using improved generalized normal distribution algorithm. 9, (9), p. 995.

Abdelghany, R.Y., Kamel, S., Sultan, H.M., Khorasy, A., Elsayed, S.K., Ahmed, M., 2021. Development of an improved bonobo optimizer and its application for solar cell parameter estimation. Sustainability 13 (7), 3863. http://dx.doi.org/10.3390/SU13073863.

Abdollahzadeh, B., Gharehchopogh, F.S., Mirjalili, S., 2021a. Artificial gorilla troops optimizer: A new nature-inspired metaheuristic algorithm for global optimization problems. Int. J. Intell. Syst. 36 (10), 5887–5958.

Abdollahzadeh, B., et al., 2021b. African vultures optimization algorithm: A new nature-inspired metaheuristic algorithm for global optimization problems. 158, 107408.

Aboagye, B., Gyamfi, S., Ofosu, E.A., Djordjevic, S., 2022. Investigation into the impacts of design, installation, operation and maintenance issues on performance and degradation of installed solar photovoltaic (PV) systems. Energy Sustain. Dev. 66, 165–176. http://dx.doi.org/10.1016/J.ESD.2021.12.003.

Askarzadeh, A., Rezazadeh, A., 2012. Parameter identification for solar cell models using harmony search-based algorithms. Sol. Energy 86 (11), 3241–3249. http://dx.doi.org/10.1016/J.SOLENER.2012.08.018.

Ayyarao, T.S.L.V., Kumar, P.P., 2022. Parameter estimation of solar PV models with a new proposed war strategy optimization algorithm. Int. J. Energy Res. http://dx.doi.org/10.1002/ER.7629.

Bisht, R., Sikander, A., 2022. A novel way of parameter estimation of solar photovoltaic system. COMPEL - Int. J. Comput. Math. Electr. Electron. Eng. 41 (1), 471–498. http://dx.doi.org/10.1108/COMPEL-05-2021-0166/FULL/PDF.

Biswas, P.P., Suganthan, P.N., Wu, G., Amaratunga, G.A.J., 2019. Parameter estimation of solar cells using datasheet information with the application of an adaptive differential evolution algorithm. Renew. Energy 132, 425–438. http://dx.doi.org/10.1016/J.RENENE.2018.07.152.

Burghard, U., Dütschke, E., Caldes, N., Oltra, C., 2022. Cross-border concentrated solar power projects - opportunity or dead end? A study into actor views in Europe. Energy Policy 163, 112833. http://dx.doi.org/10.1016/J.ENPOL.2022.112833.

Chen, X., Xu, B., Mei, C., Ding, Y., Li, K., 2018. Teaching–learning–based artificial bee colony for solar photovoltaic parameter estimation. Appl. Energy 212, 1578–1588. http://dx.doi.org/10.1016/J.APENERGY.2017.12.115.

DIab, A.A.Z., Sultan, H.M., Do, T.D., Kamel, O.M., Mossa, M.A., 2020. Coyote optimization algorithm for parameters estimation of various models of solar cells and PV modules. IEEE Access 8, 111102–111140. http://dx.doi.org/10.1109/ACCESS.2020.3000770.

Djanssou, D.M., Dadjé, A., Djongyang, N., Estimation of photovoltaic cell parameters using the honey badger algorithm. Int. J. Eng. Adv. Technol. (IJEAT), 105-108.

Düzenli, T., Onay, F.K., Aydemir, S.B., 2022. Improved honey badger algorithms for parameter extraction in photovoltaic models. Optik 169731. http://dx.doi.org/10.1016/j.ijleo.2022.169731.

El-Dabah, M.A., et al., 2021. Parameter estimation of triple diode photovoltaic model using an artificial ecosystem-based optimizer. 31, (11), e13043.

Eltamaly, A.M., 2022. Musical chairs algorithm for parameters estimation of PV cells. Sol. Energy 241, 601–620. http://dx.doi.org/10.1016/j.solener.2022.06.043.

Fan, Y., et al., 2022. Random reselection particle swarm optimization for optimal design of solar photovoltaic modules. 239, 121865.

Faramarzi, A., et al., 2020. Marine predators algorithm: A nature-inspired metaheuristic. Expert Syst. Appl. 113377.

Gandomi, A.H.J.I.t., 2014. Interior search algorithm (ISA): a novel approach for global optimization. 53, (4), pp. 1168–1183.

Gawusu, S., Zhang, X., Ahmed, A., Jamatutu, S.A., Miensah, E.D., Amadu, A.A., Osei, F.A.J., 2022. Renewable energy sources from the perspective of blockchain integration: From theory to application. Sustain. Energy Technol. Assess. 52, 102108. http://dx.doi.org/10.1016/J.SETA.2022.102108.

Ginidi, A.R., et al., 2021. Supply demand optimization algorithm for parameter extraction of various solar cell models. 7, pp. 5772–5794.

Gong, W., Cai, Z., 2013. Parameter extraction of solar cell models using repaired adaptive differential evolution. Sol. Energy 94, 209–220.

Jiao, S., Chong, G., Huang, C., Hu, H., Wang, M., Heidari, A.A., Chen, H., Zhao, X., 2020. Orthogonally adapted harris hawks optimization for parameter estimation of photovoltaic models. Energy 203, 117804. http://dx.doi.org/10.1016/J.ENERGY.2020.117804.

Jordehi, A.R., 2016. Parameter estimation of solar photovoltaic (PV) cells: A review. Renew. Sustain. Energy Rev. 61, 354–371. http://dx.doi.org/10.1016/J.RSER.2016.03.049.

Kumar, C., Mary, D.M., 2022. A novel chaotic-driven tuna swarm optimizer with Newton–raphson method for parameter identification of three-diode equivalent circuit model of solar photovoltaic cells/modules. Optik 169379. http://dx.doi.org/10.1016/j.ijleo.2022.169379.

Lekouaghet, B., Boukabou, A., Boubakir, C., 2021. Estimation of the photovoltaic cells/modules parameters using an improved Rao-based chaotic optimization technique. Energy Convers. Manage. 229, 113722. http://dx.doi.org/10.1016/J.ENCONMAN.2020.113722.

Li, S., Gong, W., Yan, X., Hu, C., Bai, D., Wang, L., 2019. Parameter estimation of photovoltaic models with memetic adaptive differential evolution. Sol. Energy 190, 465–474. http://dx.doi.org/10.1016/J.SOLENER.2019.08.022.

Liang, J., Ge, S., Qu, B., Yu, K., Liu, F., Yang, H., Li, Z., 2020. Classified perturbation mutation based particle swarm optimization algorithm for parameters extraction of photovoltaic models. Energy Convers. Manage. 203, 112138. http://dx.doi.org/10.1016/j.enconman.2019.112138.

Mi, X., Liao, Z., Li, S., Gu, Q., 2021. Adaptive teaching–learning-based optimization with experience learning to identify photovoltaic cell parameters. Energy Rep. 7, 4114–4125. http://dx.doi.org/10.1016/J.EGYR.2021.06.097.

Mirjalili, S.J.K.-b.s., 2016. SCA: a sine cosine algorithm for solving optimization problems. 96, pp. 120–133.

Mirjalili, S., Mirjalili, S.M., Lewis, A., 2014. Grey wolf optimizer. Adv. Eng. Softw. 69, 46–61.

Naeijian, M., Rahimnejad, A., Ebrahimi, S.M., Pourmousa, N., Gadsden, S.A., 2021. Parameter estimation of PV solar cells and modules using Whippy Harris Hawks Optimization Algorithm. Energy Rep. 7, 4047–4063. http://dx.doi.org/10.1016/J.EGYR.2021.06.085.

Nguyen, T.T., Nguyen, T.T., Tran, T.N., 2022. Parameter estimation of photovoltaic cell and module models relied on metaheuristic algorithms including artificial ecosystem optimization. Neural Comput. Appl. 1–26. http://dx.doi.org/10.1007/s00521-022-07142-3.

Nunes, H., et al., 2018. A new high performance method for determining the parameters of PV cells and modules based on guaranteed convergence particle swarm optimization. Appl. Energy 211, 774–791.

Rezk, H., et al., 2021. Optimal parameter estimation of solar PV panel based on hybrid particle swarm and grey wolf optimization algorithms. 6, (6).

Şevik, S., Aktaş, A., 2022. Performance enhancing and improvement studies in a 600 kW solar photovoltaic (PV) power plant; manual and natural cleaning, rainwater harvesting and the snow load removal on the PV arrays. Renew. Energy 181, 490–503. http://dx.doi.org/10.1016/J.RENENE.2021.09.064.

Shankar, N., Saravanakumar, N., Indu Rani, B., 2020. Solar photovoltaic module parameter estimation with an enhanced differential evolutionary algorithm using the manufacturer's datasheet information. Optik 224, 165700. http://dx.doi.org/10.1016/J.IJLEO.2020.165700.

Sharma, A., Sharma, A., Dasgotra, A., Jately, V., Ram, M., Rajput, S., Averbukh, M., Azzopardi, B., 2021. Opposition-based tunicate swarm algorithm for parameter optimization of solar cells. IEEE Access 9, 125590–125602. http://dx.doi.org/10.1109/ACCESS.2021.3110849.

Singh, A., Sharma, A., Rajput, S., Bose, A., Hu, X., 2022. An investigation on hybrid particle swarm optimization algorithms for parameter optimization of PV cells. Electronics 11 (6), 909. http://dx.doi.org/10.3390/electronics11060909.

Soliman, M.A., Hasanien, H.M., Alkuhayli, A.J.I.A., 2020. Marine predators algorithm for parameters identification of triple-diode photovoltaic models. 8, 155832-155842.

Tan, Y.T., Kirschen, D.S., Jenkins, N., 2004. A model of PV generation suitable for stability analysis. IEEE Trans. Energy Convers. 19 (4), 748–755. http://dx.doi.org/10.1109/TEC.2004.827707.

Xiong, G., Li, L., Mohamed, A.W., Yuan, X., Zhang, J., 2021. A new method for parameter extraction of solar photovoltaic models using gaining–sharing knowledge based algorithm. Energy Rep. 7, 3286–3301. http://dx.doi.org/10.1016/J.EGYR.2021.05.030.

Xiong, G., et al., 2018. Parameter extraction of solar photovoltaic models using an improved whale optimization algorithm. 174, pp. 388–405.

Xu, S., Wang, Y., 2017. Parameter estimation of photovoltaic modules using a hybrid flower pollination algorithm. Energy Convers. Manage. 144, 53–68. http://dx.doi.org/10.1016/J.ENCONMAN.2017.04.042.

Zhang, Y., Jin, Z., Mirjalili, S., 2020. Generalized normal distribution optimization and its applications in parameter extraction of photovoltaic models. Energy Convers. Manage. 224, 113301.

Zhou, W., Wang, P., Heidari, A.A., Zhao, X., Turabieh, H., Mafarja, M., Chen, H., 2021. Metaphor-free dynamic spherical evolution for parameter estimation of photovoltaic modules. Energy Rep. 7, 5175–5202. http://dx.doi.org/10.1016/J.EGYR.2021.07.041.